



Title	A Review of El Niño Southern Oscillation Linkage to Strong Volcanic Eruptions and Post-Volcanic Winter Warming
Author(s)	Dogar, Muhammad Mubashar; Hermanson, Leon; Scaife, Adam A.; Visioni, Daniele; Zhao, Ming; Hoteit, Ibrahim; Graf, Hans-F.; Dogar, Muhammad Ahmad; Almazroui, Mansour; Fujiwara, Masatomo
Citation	Earth Systems and Environment, 7(1), 15-42 <a href="https://doi.org/10.1007/s41748-022-00331-z">https://doi.org/10.1007/s41748-022-00331-z</a>
Issue Date	2022-11-07
Doc URL	<a href="http://hdl.handle.net/2115/90646">http://hdl.handle.net/2115/90646</a>
Rights	This version of the article has been accepted for publication, after peer review (when applicable) and is subject to Springer Nature 's AM terms of use, but is not the Version of Record and does not reflect post-acceptance improvements, or any corrections. The Version of Record is available online at: <a href="http://dx.doi.org/10.1007/s41748-022-00331-z">http://dx.doi.org/10.1007/s41748-022-00331-z</a>
Type	article (author version)
File Information	Dogareta2022-Review-ENSO-Volcanism-Final.pdf



[Instructions for use](#)

1 **A Review of El Niño Southern Oscillation Linkage to Strong Volcanic Eruptions and Post-**  
2 **Volcanic Winter Warming**

3 Muhammad Mubashar Dogar<sup>1,2,\*</sup>, Leon Hermanson<sup>3</sup>, Adam A. Scaife<sup>3,4</sup>, Daniele Visioni<sup>5</sup>, Ming  
4 Zhao<sup>6</sup>, Ibrahim Hoteit<sup>7</sup>, Hans-F. Graf<sup>8</sup>, Muhammad Ahmad Dogar<sup>9</sup>, Mansour Almazroui<sup>10,11</sup>,  
5 Masatomo Fujiwara<sup>2</sup>  
6

7 **ABSTRACT**

8 Understanding the influence of volcanism on ENSO and associated climatic impacts is of great  
9 scientific and social importance. Although many studies on the volcano-ENSO nexus are available,  
10 a thorough review of ENSO sensitivity to explosive eruptions is still missing. Therefore, this study  
11 aims to provide an in-depth assessment of the ENSO response to volcanism. Most past studies  
12 suggest that there is an emerging consensus in models, with the vast majority showing an El Niño–  
13 like SST response during the eruption year and a La Niña–like response a few years later. RCP8.5-  
14 based climate model projections also suggest strong El Niño conditions and significant monsoonal  
15 rainfall reduction following strong tropical volcanism. However, some studies involving climate  
16 reconstructions and model simulations still raise concerns about the ENSO-volcano link and  
17 suggest a weak ENSO response to volcanism. This happens because ENSO response to volcanism  
18 seems very sensitive to reconstruction methods, ENSO preconditioning, eruption timing, position  
19 and amplitude. We noticed that some response mechanisms are still unclear; for instance, how the  
20 tropical volcanic forcing with nearly uniform radiative cooling projects onto ENSO when  
21 coincidental ENSO events are underway. Moreover, there are fewer observational and proxy  
22 records for extratropical volcanism impact on ENSO. Nevertheless, model-based studies suggest  
23 that Northern (Southern) Hemispheric extratropical eruption may lead to an El Niño (La Niña)–like  
24 response. We further noticed that the origin of post-eruption winter warming is still elusive,  
25 however, recent findings suggest that the large-scale circulation changes concurrently occurring  
26 during volcanism are the potential source of high-latitude winter warming. Existing uncertainties in  
27 the simulated ENSO response to volcanism could be improved by considering a synchronized  
28 modeling approach with large ensembles.  
29

30 **Key words:** Tropical Volcanism, Extratropical Volcanism, El Niño–Southern Oscillation (ENSO),  
31 General Circulation Models, Observations, Climate Proxies.

- 32  
33 1. Global Change Impact Studies Centre, Ministry of Climate Change, Islamabad, Pakistan  
34 2. Faculty of Environmental Earth Science, Hokkaido University, Sapporo, Japan  
35 3. Met Office Hadley Centre, Exeter, United Kingdom  
36 4. College of Engineering, Mathematics and Physical Sciences, Exeter University, Exeter, United  
37 Kingdom  
38 5. Sibley School of Mechanical and Aerospace Engineering, Cornell University, Ithaca, New York,  
39 USA  
40 6. NOAA Geophysical Fluid Dynamics Laboratory, Princeton, New Jersey, USA  
41 7. Physical Sciences and Engineering Division, King Abdullah University of Science and Technology  
42 (KAUST), Thuwal 23955-6900, Saudi Arabia  
43 8. Centre for Atmospheric Science, University of Cambridge, Cambridge, United Kingdom  
44 9. Department of Computer Science and Information Technology, University of Lahore, Pakistan  
45 10. Center of Excellence for Climate Change Research/Department of Meteorology, King Abdulaziz  
46 University, Jeddah, Saudi Arabia  
47 11. Climatic Research Unit, School of Environmental Sciences, University of East Anglia, Norwich,  
48 United Kingdom

49  
50 \*mubashardogar@yahoo.com, Phone: +81-08045071566  
51  
52

## 1 **1. Introduction**

2 The El Niño–Southern Oscillation (ENSO) shapes global climate patterns yet its sensitivity to  
3 external forcing remains ambiguous. Modeling studies suggest that ENSO is sensitive to sulfate  
4 aerosols associated with explosive volcanism but observational support for this effect remains  
5 uncertain. This paper reviews the current state of knowledge of volcanic eruptions and its impacts  
6 on ENSO variability, using proxy reconstructions and recent modeling results from state-of-the-art  
7 global climate models. The primary focus in this review is to discuss latest progress and consensus  
8 on the impacts of strong tropical and extratropical eruptions on ENSO, whose variability has  
9 tremendous economic and societal impacts.

10 It is well known that the large volcanic eruptions produce profound global and regional  
11 influences by affecting both the atmosphere and ocean circulation (Robock, 2000, Driscoll et al.  
12 2012; Stenchikov et al. 2006, 2009; Ding et al. 2014; Fujiwara et al. 2015, 2020; Dogar et al. 2017;  
13 Swingedouw et al. 2017; Dogar, 2018; Dogar and Sato, 2019; McGregor et al. 2020). Climatic  
14 impacts of explosive volcanic eruptions include a temporary disruption of global surface warming  
15 due to their strong surface temperature cooling effects (Fyfe et al. 2013; Haywood et al. 2014;  
16 Santer et al. 2014; Maher et al. 2015; Medhaug et al. 2017, Monerie et al. 2017). Large explosive  
17 eruptions potentially inject immense sulfur-containing gases, ash and sulfur rich aerosols into the  
18 lower part of the stratosphere, where they surround the globe through circulation. These volcanic  
19 aerosol particles scatter and absorb incoming solar radiation, resulting in a net reduction in surface  
20 radiation leading to net surface cooling, and heating of the lower stratosphere (Luther, 1976;  
21 Rampino & Self, 1984; Stenchikov et al. 1998; Robock & Mao, 1995; Timmreck, 2012;). Global  
22 mean surface temperatures reach maximum cooling within a few months after the eruptions peak in  
23 optical depth and get back to normal a couple of years after the event (e.g., Thompson et al. 2009;  
24 Timmreck, 2012; Folland et al 2018).

25 The largest volcanic eruptions also lead to a reduction in ocean heat content and drop in sea  
26 level (Church et al. 2005; Pausata et al. 2015; Fasullo et al. 2017; Dogar and Sato, 2020; Ding et al.  
27 2014; Dogar and Shahid, 2020). Volcanic eruptions could also potentially modulate natural climate  
28 variability, as they provide suitable conditions in the lower stratosphere leading to the Arctic  
29 Oscillation positive phase during the first two boreal winters after eruption (Kodera, 1994;  
30 Christiansen, 2008; Marshall et al. 2009; Shindell et al. 2004; Stenchikov et al. 2006). Given that El  
31 Niño tends to be associated with a negative phase of the North Atlantic Oscillation (NAO), there is  
32 also a possibility that post-eruption ENSO variability influences the global volcanic response  
33 through stratospheric pathways (Marshall et al. 2009; Ineson and Scaife, 2009; King et al. 2018).

34 Recently, several studies have strengthened the case for impacts of volcanic eruptions on  
35 the El Niño–Southern Oscillation (e.g., McGregor & Timmermann, 2011; Zanchettin et al. 2012;  
36 Predybaylo et al. 2017, 2020; Hermanson et al. 2020; Pausata et al. 2020; Yang et al. 2022) and if

1 ENSO modulation by volcanic events is strong, it may likely enhance our understanding on the  
2 predictability of El Niño/La Niña events after future volcanic eruptions. Given the strong ENSO  
3 influence on global and regional climate and its strong societal importance, we therefore review the  
4 current evidence associated with the impact of strong volcanism on ENSO.

5 Analysis of observational Sea Surface Temperature (SST) and surface air temperature  
6 suggests that El Niño events overlapped with four large eruptions that occurred in the recent  
7 historical period (Figure 1 and Figure 2). MacCracken and Luther (1984) first identified the  
8 apparent connection between volcanism and ENSO (i.e., an El Niño type event develops within a  
9 few seasons after El Chichón type forcing) using statistical dynamical climate model, which latter  
10 was supported by Handler (1984, 1986, 1989). However, the relationship shown in Handler (1984,  
11 1989) was mainly based on serial correlations between both phenomena that appeared in observed  
12 SST anomalies composited around volcanic events (Figure 1). A detailed initial review of volcano-  
13 El Niño hypothesis, mainly based on statistical correlation methods, could be seen in past studies  
14 (e.g., Mass and Portman, 1989; Handler and Andsager, 1994; Adams et al. 2003). Questions about  
15 Handler's (1984) results arose due to the methodology used to study statistical robustness, volcanic  
16 chronology, and volcanic events timing relative to the onset of ENSO event (e.g., Sear et al. 1987;  
17 Nicholls, 1988; Handler 1989; Handler and Andsager, 1994; Self et al. 1997; Robock, 2000;  
18 Stevenson et al. 2017). This is obvious in Figure 1a, as both the 1982 El Chichón and 1991  
19 Pinatubo volcanic eruptions happened after the onset of El Niño events in the relevant years,  
20 suggesting a coincidental relationship. However, this could also be related to ENSO  
21 preconditioning and its linkage to volcanic forcing (Predybaylo et al. 2020; Zhu et al. 2022).

22 Xing et al. (2020) examined the composite global surface air temperature (SAT) anomalies  
23 during the first boreal winter after five 20th Century eruptions in the reanalysis and GISS Surface  
24 Temperature (GISTEMP) observations. Both in 20th Century Reanalysis version 2c (20CRv2c;  
25 Figure 2a) and observations (GISTEMP; Fig 2b), a pause in post-eruption global cooling during the  
26 first boreal winter appeared due to significant El Niño-like warming in the tropics and strong  
27 warming in Eurasia, which is consistent with previous finding (Robock and Mao 1992).

28 Similarly, by using observational and modeling studies, Chai et al. (2020) also studied the  
29 apparent ENSO link to 20th Century large tropical eruptions. In observational records of the Agung  
30 in 1963, El Chichon in 1982, and Pinatubo in 1991 eruptions, the El Niño peak occurred in the first  
31 winter after each eruption (Figure 3). Following aforementioned three tropical eruption events,  
32 westerly anomalies over western-to-central equatorial Pacific (WCEP) emerged before the peak of  
33 the El Niño phase. However, relying on three cases only, it cannot be concluded that these westerly  
34 anomalies are caused by tropical eruptions, as the coincidental occurrence could occur simply due  
35 to unrelated internal variability (Self et al. 1997; Robock et al. 1995; Menegoz et al. 2018).  
36 However, Chai et al. (2020) took composites of the community earth system model (CESM) large

1 ensemble (CESM-LE) experiment with 41 ensemble members and using a large ensemble mean to  
2 reduce internal variability, reproduced the El Niño response during the second winter following  
3 these three eruptions individually (Figure 3). Prior to the peak El Niño phase in the year of the  
4 eruption; a significant westerly anomaly from WCEP is modeled for each eruption. El Niño then  
5 develops and reaches its peak in the second northern winter. Figure 3 further suggests a weak La  
6 Niña-like response in the observations at year (2) and the CESM-LE simulation at year (3),  
7 especially for the Agung and El Chichon eruptions. This La Niña-like response largely resembles  
8 the results of Maher et al. (2015) who analyzed CMIP5 models and showed a La Niña-like  
9 response a couple of years after the large tropical eruption events. These La Niña-like responses  
10 have also been suggested by other researchers (e.g., Li et al. 2013; Pausata et al. 2015). Although  
11 this transition to La Niña-like responses is argued to be dynamically driven rather than a direct  
12 consequence of general post-eruption cooling (Pausata et al. 2016), the underlying mechanism for  
13 these rapid eruption-induced El Niño transitions to La Niña needs further investigation.

14         The current idea encompassing the volcanism influence on ENSO has evolved from the  
15 forerunner hypothesis suggesting that volcanism has the tendency to modulate the probability and/or  
16 intensity of ENSO activity, however, a clear understanding of this relationship is still obscure.  
17 Therefore, the rationale behind the present review article is to summarize our understanding of how  
18 volcanic eruptions occurring in the tropics and extratropics may influence ENSO forcing using up-  
19 to-date literature on climate proxies, and climate model simulations. This summary will include a  
20 discussion about how ENSO modulation could occur following strong tropical and extratropical  
21 volcanism. The sensitivity of the results to eruption magnitude and timing will also be reviewed  
22 keeping in mind ENSO preconditioning at the time of the eruption. In addition, we will also review  
23 the mysterious post-volcanic high-latitude winter warming effects on Eurasia and North America.  
24 The rest of this review article is organized as follows: Section 2 and 3 present the details of the  
25 ENSO and volcanic forcing respectively. Section 4 discusses the volcano influence on ENSO from  
26 paleoclimate proxy evidence, while Section 5 outlines volcano influence on ENSO from model-  
27 based studies. Key underlying mechanisms suggested so far to understand the influence of volcanic  
28 forcing on ENSO are also analyzed and reviewed in Section 5, whereas Section 6 highlights the  
29 sensitivity of ENSO and volcanism to ocean circulation. Section 7 reviews in detail the potential  
30 role of ENSO preconditioning, eruption seasonality, position and magnitude in the ENSO response  
31 mechanism. Post-eruption high-latitude winter warming effects are discussed in Section 8.  
32 Summary and concluding remarks on volcano-ENSO linkage are briefly discussed in Section 9 and  
33 Section 10.

## 34 **2. ENSO**

35         El Niño–Southern Oscillation (ENSO) is one among the prominent interannual climate  
36 fluctuations on Earth (McPhaden et al., 2006) observed through alternating warm and cold SST

1 conditions in the tropical Pacific (Trenberth et al. 1998; Timmermann et al. 1999; Yeh et al. 2018)  
2 and is considered one of the main driver of ocean and the atmospheric climate variability. ENSO  
3 variability has the potential to produce extreme events (e.g., droughts, floods) and variations in  
4 cyclone activity through global scale atmospheric teleconnections (Nicholls, 1985; Trenberth et al.  
5 1998; Power et al. 1999; Dogar and Almazroui, 2022). The climatic impacts of ENSO variability  
6 and its intensity on global and regional temperature, precipitation, pressure and associated wind  
7 have been extensively discussed in several studies (e.g., Timmermann et al. 1999; Ashok et al.  
8 2007; Zhang et al. 2013; Zhang et al. 2015; Dogar et al. 2019). Similarly, the direct radiative impact  
9 of volcanism on global and regional climate is also discussed in detail in several studies (Robock,  
10 2000; Haywood et al. 2013; Dogar et al. 2017). However, ENSO linkage to volcanic activity is not  
11 explored much and limited research has been conducted in this direction.

12 In recent studies it has been shown that the volcanic forcing may trigger El Niño-like  
13 temperature anomalies in winter and summer seasons following volcanism. For instance, Dogar and  
14 Sato (2019) used statistical methods to emphasize that the ENSO has a significantly high  
15 correlation with regional surface temperatures in winter and summer, implying that it plays a  
16 significant role to modulate regional climate. Several other studies also pointed out that an El Niño  
17 event could potentially modify a volcanic signal especially in winter (Robock and Mao, 1995,  
18 Timmreck, 2012; Dogar et al. 2017). Typically, an ENSO event peaks during winter period, but its  
19 evolution could start a year before its peak and subsequent decay could extend around one to two  
20 years after the peak period, hence it has the tendency to interact with a volcanic signal during the  
21 summer season as well. For instance, Northern Hemisphere (NH) high-latitude volcanic eruptions  
22 force an El Niño along with southward shift of the ITCZ within the following 8–9 months during  
23 the summer (Haywood et al. 2013; Pausata et al. 2015, 2016). Moreover, tropical low-latitude  
24 explosive eruption events tend to develop El Niño-like anomalies for about one year after the  
25 eruption (Adams et al. 2003; Mann et al. 2005; Maher et al. 2015; Ohba et al. 2013; Predybaylo et  
26 al. 2017). Since the last three major tropical volcanic eruptions (i.e., Agung in 1963, El Chichón in  
27 1982, and Pinatubo in 1991) overlapped with El Niño episodes (Trenberth and Dai, 2007;  
28 Timmreck, 2012); thus, the volcanic impacts could be hampered or masked by ENSO impacts.  
29 Hence, to precisely assess the volcanic impacts, the removal of ENSO signals (for instance, by  
30 using linear regression or superposed epoch analysis) was suggested in past studies (e.g., Sear et al.  
31 1987; Mass and Portman, 1989; Dogar et al. 2017; Robock and Liu, 1994). However, recent studies  
32 suggest that the ENSO signal could be modulated by volcanism and vice versa (through post-  
33 volcanic indirect circulation effects), therefore, ENSO and volcanic signals need to be studied in  
34 conjunction to each other (Dogar and Sato, 2019). Therefore, in this review paper, we revisited  
35 climate proxies and past modeling studies to better understand the volcano-ENSO linkages.

36

1

### 2 **3. Volcanism**

3 Our understanding of the microphysical and chemical processes of volcanic aerosols and their effect  
4 on climate is still incomplete largely because of small number of massive stratospheric eruptions  
5 occurring in the satellite era. Volcanic eruptions potentially inject a massive amount of sulfur rich  
6 gases into the lower part of the stratosphere, where they are oxidized, forming sulfate aerosol plume  
7 that disturb the earth radiative balance by scattering the incoming solar shortwave (SW) radiation,  
8 and absorption of infrared (IR) radiation (Robock, 2000; Stenchikov et al. 1998; Santer et al. 2014).  
9 This disruption of the Earth's energy budget by volcanic forcing can persist for two to three years  
10 (Robock, 2000), contingent on the lifespan of stratospheric aerosols and may extend longer due to  
11 effects on stratospheric water vapor (Joshi and Shine, 2003; Soden et al. 2002).

12 Although the volcanic radiative forcing has short life, its large spatial scale and magnitude  
13 make it an important driver of climate variability as it strongly interacts with Earth's radiative  
14 Energy budget (Timmreck et al. 2009; Timmreck, 2012). Therefore, strong eruptions cause a  
15 reduction in the global surface temperature that can remain for several years following these events,  
16 resulting in variations in ocean temperature, sea level and circulation changes that can last for  
17 decades (Church et al. 2005; Stenchikov et al. 2009; Dogar et al. 2020; Dogar and Stenchikov,  
18 2013). This makes them an important part of the climate system, regardless of their short  
19 stratospheric lifetime (Robock, 2000; Timmreck, 2012). It is, however, challenging to untangle the  
20 volcanic impact of individual eruptions at regional scales due to multiple coincident climate  
21 phenomena, such as the monsoon circulation and other interfering climate variability modes whose  
22 regional climate impacts could be much higher compared to global mean variations caused by the  
23 eruption (Liu et al. 2022; Dogar et al. 2017; Fischer et al. 2007; Fasullo et al. 2019; Singh et al.  
24 2020; Tejedor et al. 2021; Zuo et al. 2021).

25 While the recent volcanic events (e.g., El Chichon and Pinatubo) have been well observed  
26 (and forcing effects are well replicated in models), the limited observational data for past volcanic  
27 eruptions leads to large uncertainties and biases in the aerosol particle size, hemispheric  
28 distributions, and radiative forcing estimates (Stenchikov et al. 2004; Santer et al. 2014; Toohey et  
29 al. 2011; Raible et al. 2016; Marshall et al. 2021, 2022). The latest climate models with interactive  
30 volcanic aerosols have been shown to effectively simulate the aerosol loading, size distribution and  
31 associated climate response following the Pinatubo eruption (Mills et al. 2016; Niemeier et al.  
32 2010; Mills et al. 2017). However, very less data exists to constrain other eruptions of different  
33 extents, latitudes, and seasonality. Several recent model studies suggested that the eruption latitude,  
34 altitude, strength, and season of occurrence, could induce differences in the aerosol evolution,  
35 loading (e.g., Toohey et al. 2011; Kravitz & Robock, 2011), and climate responses (Zhuo et al.  
36 2021). The differences in radiative impacts of volcanic eruptions that occurred at different latitudes

1 (i.e., tropical and extratropical eruptions) are clearly emphasized (Haywood et al. 2013; Pausata et  
2 al. 2015; Liu et al. 2018; Zhuo et al. 2021). Aerosols produced from strong tropical eruptions often  
3 surround the entire globe, whereas aerosols from mid-to-high-latitude eruptions are confined to the  
4 hemisphere of eruption (Oman et al. 2005; Kravitz & Robock, 2011). Even for tropical eruptions,  
5 the dispersion depends on the phase of internal variability such as the Quasi-Biennial Oscillation  
6 (Trepte et al. 1993; Jones et al. 2016). Simulations also suggest that an eruption similar to Pinatubo  
7 occurring in northern winter will cause significantly greater global cumulative aerosol loading than  
8 a similar eruption occurring at any other time of the year (e.g., Stevenson et al. 2017; Toohey et al.  
9 2011; Stoffel et al. 2015). Similarly, for the Northern Hemisphere (NH) high-latitude eruptions of  
10 similar magnitude, the largest aerosol loading is obtained for eruptions occurring in summer than in  
11 winter (Toohey et al. 2011; Kravitz & Robock, 2011). This strongly suggests that aerosol size,  
12 distribution, lifetime, and accompanying climatic effects appear to be dependent on the  
13 meteorological state, the eruption season, the latitude, and strength of eruption.

14 Numerous model simulations, observations and hemispheric temperature reconstructions  
15 have been used so far to evaluate the climatic impacts of the major volcanic events. However,  
16 volcanically induced cooling derived from model simulations is effectively much higher than the  
17 cooling visualized in reconstructions (Mann et al. 2012; Büntgen et al. 2014; Stoffel et al. 2015)  
18 with some exceptions following El Chichon and Pinatubo tropical eruptions where strong regional  
19 cooling is seen in observation compared to high-resolution atmospheric model (HiRAM)  
20 simulations (e.g., Dogar et al. 2017). It suggests that either the modeled forcing is unrealistically  
21 high or the proxies underestimate cooling (Anchukaitis et al. 2012; Mann et al. 2012; Stoffel et al.  
22 2015; Dee and Steiger, 2022) and/or the model cooling response is overestimated (Chylek et al.  
23 2020; Stoffel et al. 2015; Marshall et al. 2021), perhaps due to a weak response in the Arctic  
24 Oscillation and hence a lack of winter warming (Stenchikov et al. 2006; Marshall et al. 2009;  
25 Driscoll et al. 2012; Zambri et al. 2017). Alternatively, support for excessive model forcing is  
26 indicated by the results of numerous studies showing that there is no general relationship between  
27 the extent of forcing and the global mean temperature response (e.g., Timmreck et al. 2009; Bader  
28 et al. 2020). This is related with the microphysical processes of volcanic aerosols including its  
29 interaction with volcanic ash that effectively limit the impact of strong volcanic eruptions (Zhu et  
30 al. 2021). In particular, while considering past eruptions, fixing the concentration and size  
31 distribution of aerosols does not give a realistic and accurate simulation of the eruption effects, and  
32 therefore, its use can lead to inaccurate estimations of volcanism (Stoffel et al. 2015; Marshall et al.  
33 2021). Santer et al. (2014) and other studies (Dogar and Sato, 2019) suggest that agreement with  
34 observations can be improved if the contribution due to internal variability (e.g., ENSO and NAO)  
35 is accounted for. Disparities in model responses to volcanism and their inconsistency with  
36 observations and proxy-based reconstructions could also be accounted for by the contribution of



1 volcanic ash and its interaction with Sulfur Dioxide as volcanic input data used in models is missing  
2 this contribution (Zhu et al. 2021).

3 Above discussion strongly suggests that, regardless of having true estimations of observed  
4 impacts particularly for recent massive eruptions, effective modeling of the climate responses or  
5 impacts (with true magnitude) of past volcanic events remains challenging and demanding work for  
6 climate models partly because of the limited accessibility of precise input forcing data required for  
7 correct estimation of radiative forcing even before taking into account model errors (Marshall et al.  
8 2021). Therefore, precise information for past and future eruptions about the time of eruption (i.e.,  
9 eruption season), latitude, particle microphysics, and size distribution is highly needed to test  
10 whether models can realistically replicate accurate response magnitudes (e.g., Zhuo et al. 2021; Zhu  
11 et al. 2021; Marshall et al. 2021).

#### 12 **4. Assessment of Volcano-ENSO Linkages using Climate Proxy Records**

13 Several climate proxy datasets are available that detail the dates and strength of past historical  
14 eruptions (e.g., Sigl et al. 2015; Gao et al. 2008; Crowley et al. 2008). We noticed that these  
15 datasets differ in inception of eruption dates (i.e., starting year). This is because the volcanic dates  
16 in Sigl et al. (2015) and Gao et al. (2008) datasets correspond to global estimates of volcanic  
17 radiative forcing, while for the case of Crowley et al. (2008), volcanic dates correspond to the  
18 tropical estimates (averaged over 30°S-30°N) of radiative forcing. It is believed that the volcanic  
19 eruptions contribute greatly to climate variability, but quantifying these contributions is limited due  
20 to inconsistencies in the timing of volcanic aerosol loading and subsequent cooling signatures.  
21 Earlier studies have revealed that ENSO's response and sensitivity to eruptions over the past  
22 millennium appears to be significant, while important uncertainties remain (e.g. Raible et al. 2016;  
23 Dee et al. 2020; Hernandez et al. 2020; Zhu et al. 2021, 2022). Some studies suggest that a strong  
24 El Niño-like SST anomalous pattern occurs during eruption year that could persist for subsequent  
25 years, as shown in the observed 350 years (1649-2000) record (Adams et al. 2003). Contrary to this,  
26 other studies propose that tropical volcanism may trigger a La Niña-like response, particularly at  
27 longer lead times (Anchukaitis et al. 2010; Li et al. 2013; Maher et al. 2015; Pausata et al. 2015).  
28 There is also inconsistency among paleo-reconstructions regarding the magnitude representing  
29 increased likelihood of an El Niño episode in the years that follows major eruption events  
30 (Stevenson et al. 2017). We noticed that various paleoclimate studies are conducted so far to  
31 reconstruct ENSO variability of past events and mostly they show varying results. For instance, Dee  
32 and Steiger, (2022) tested the volcanism-ENSO linkage in the past 2000 years long records of Paleo  
33 Hydrodynamics Data Assimilation (PHYDA) product and noticed a weak tropical Pacific response  
34 following large tropical volcanism resembling to El Niño. These results were also not significant (at  
35 95% confidence) when evaluated using superposed epoch analysis (SEA) and self-organizing maps.  
36 Significant results emerged when probability density functions were employed, suggesting that

1 SEA approach (i.e., composite averaging) seems less sensitive to capture an ENSO response in the  
2 presence of strong internal variability. Moreover, inconsistencies were noticed in magnitudes and  
3 spatial patterns between climate models and PHYDA regarding ENSO-volcano linkage. This study  
4 also suggests that current climate models apparently overestimate ENSO response to volcanism. We  
5 further noticed that the paleo-reconstructions also disagree on the magnitude of increased likelihood  
6 of an El Niño episode during the years that follows major eruptions. Moreover, due to the lack of  
7 observational data for comparison, it is impossible to find the best ENSO reconstruction. A careful  
8 analysis of these reconstruction studies reveal that the difference in reconstruction methods and  
9 input source data resulted in each study producing different ENSO reconstructions and hence  
10 different conclusions (Nicholls, 1988; Tierney et al. 2015; Lee et al. 2013; Braganza et al. 2009;  
11 Emile-Geay et al. 2013a, 2013b; Dee and Steiger, 2022).

12 Fadnavis et al. (2021) showed that during 1871-2016 period, 49% (26 out of 53) of the records  
13 of moderate to large tropical eruptions were found to represent El Niño conditions within two years  
14 after the eruptions that apparently caused droughts over India as they affected Indian monsoon  
15 through weakening of Hadley circulation consistent with the earlier findings of Fadnavis et al.  
16 (2019) and Khudri et al. (2017). McGregor et al. (2020) used around 17 reconstructions of ENSO  
17 variability, and looked for a consistent response (Table 1). The significance of ENSO response in  
18 these reconstructions was computed using Monte-Carlo sampling approach. This study found that  
19 around 70% (12 out of 17) reconstructions produced a strong El Niño-like response during the  
20 eruption year, whilst none produced a La Niña-like response. It also found that in about two years  
21 after the event, 47% (8 out of 17) reconstructions produced a significant (above the 95% level) La  
22 Niña-like response. This is likely relevant to the dynamics behind the lagged La Niña-like response  
23 in the model analysis of Maher et al. (2015). Thus, these results support the idea that strong  
24 volcanic eruption may potentially generate warmer SST in the central and eastern equatorial Pacific  
25 region, followed by a La Niña-like response (one year later) due to the ENSO oscillatory nature.  
26 Using last millennium reanalysis (LMR) and data assimilation framework, Zhu et al (2022) showed  
27 no significant ENSO response to volcanism during the eruption years (i.e., year 0 and year +1;  
28 Figure 4). This is something that apparently cannot be solved by more examination of our existing  
29 paleoclimatic knowledge. Thus, further modeling experimentation and analysis is needed to better  
30 understand the contribution of dynamic modulations and proxy-related problems in making  
31 variations across reconstructions.

32

## 33 **5. Assessment of Volcano-ENSO Linkages Using Modeling Studies**

### 34 **5.1. Tropical Volcanic Eruptions**

1 There are uncertainties in predicting the impact of volcanic eruptions on the occurrence of El Niño  
2 Southern Oscillation using models, since the influence of tropical explosive volcanism is not  
3 uniformly simulated within models and large ensembles are needed to isolate forced responses from  
4 internal variability. Numerical modeling experiments conducted with selected individual models  
5 have mimicked the El Niño response (e.g., MacCracken and Luther, 1984; Ohba et al. 2013;  
6 Fadnavis et al. 2021). Early experiments conducted using coupled models of intermediate  
7 complexity produce a higher likelihood of an El Niño-like condition or the happening of El Niño  
8 events after major eruptions, showing agreement with climate proxies and observational estimates  
9 (Mann et al. 2005; Emile-Geay et al. 2008). The simplicity of the intermediate complexity coupled  
10 model (e.g., Zebiak & Cane, 1987) and the uniform volcanic forcing used in these simple models,  
11 warrant that ocean dynamics (i.e., the dynamical thermostat process) is the only process by which  
12 the forcing may project on ENSO. Nevertheless, the role of the dynamical thermostat has been  
13 argued in several recent studies (e.g., Pokarel and Sikka, 2013; Gregory et al. 2016; Adam et al.  
14 2003 2016; Noh et al. 2017; Fadnavis et al. 2019). Further studies, using coupled and more complex  
15 general circulation models (GCMs), suggest several ways of volcanic forcing projection onto ENSO  
16 (e.g., McGregor & Timmermann, 2011; Predybaylo et al. 2017, 2020; Pausata et al. 2020; Fadnavis  
17 et al. 2021). The outcomes of some of these coupled model studies imply that volcanic forcing may  
18 induce an initial cooling in the equatorial Pacific region (Zanchettin et al. 2012; McGregor &  
19 Timmermann, 2011). However, this initial cooling apparently being direct radiative response of  
20 volcanic radiative forcing, is dynamically different from a La Niña event (e.g., Stevenson et al.  
21 2017). Even with the initial instantaneous cooling response to volcanism, dynamical variables  
22 suggested El Niño-like anomalous patterns emerging about a year after the peak of the eruption  
23 (e.g., McGregor & Timmermann, 2011). Evaluation of historical coupled GCM simulations  
24 performed for Phase 3 and Phase 5 of Coupled Model Intercomparison Project (CMIP) initially  
25 proposed that volcanism and ENSO linkage across CMIP models is somehow weak (e.g.,  
26 Stenchikov et al. 2006; Driscoll et al. 2012; Ding et al. 2014), which is consistent with recent proxy  
27 studies (e.g., Dee et al. 2020; Dee and Steiger, 2022). However, numerous modeling studies  
28 conducted using CMIP5 models suggest that a strong volcanic eruption induces an El Niño-like  
29 mean response in the Pacific Ocean, suggesting an increased likelihood of El Niño events, that  
30 persist for about two years after reaching the peak optical depth of the eruption (Figure 5). The El  
31 Niño-like anomalous response of the equatorial Pacific in the year following a major tropical  
32 volcanic eruption has also been reported in other modeling studies (see, e.g., Ohba et al. 2013;  
33 Stevenson et al. 2017; Predybaylo et al. 2017; Maher et al. 2015; Khodri et al. 2017; Fadnavis et al.  
34 2021; Yang et al. 2022). Nevertheless, some recent modeling studies based on CMIP5 (Xing et al.  
35 2020), Paleoclimate Modeling Inter-comparison Project (PMIP) Phase 3, PMIP3 (Chai et al. 2020),  
36 and CMIP6 (Liu et al. 2020) failed to generate an El Niño anomalous response in the first post-

1 eruption winter and long range forecast studies continue to suggest that at least some ENSO events  
2 were already set to occur, irrespective of volcanic forcing (Menegoz et al. 2018).

3 Coupled Climate models may also be employed to study climatic responses to volcanism  
4 with varying strength, locations, and the Pacific Ocean pre-eruption initial state to help understand  
5 the dynamics of ENSO modulation (Ohba et al. 2013; Lim et al. 2016; Khodri et al. 2017;  
6 McGregor & Timmermann, 2011; Stevenson et al. 2017; Predybaylo et al. 2017; Fadnavis et al.  
7 2021). Some studies initially claimed that an eruption of Pinatubo size or larger is needed to  
8 increase the probability of a post-volcano El Niño occurring (e.g. Emile-Geay et al. 2008). A  
9 similar threshold of magnitude was also recently presented by Iwi et al. (2012) and Lim et al.  
10 (2016), whose model results showed that an El Niño-like response to large tropical eruptions occurs  
11 only after a threshold of  $15 \text{ W/m}^2$  (i.e., about two or three times greater than Pinatubo). El Niño-like  
12 post-volcanic conditions are also recently reported following strong tropical eruptions of the size of  
13 Tambora 1815 (about a full order of magnitude larger than Pinatubo), which was enhanced for  
14 future climate under RCP-8.5 climate scenario because of, enhanced moisture transport (i.e., ocean-  
15 land thermal gradient mechanism) and associated higher sensitivity to monsoon system (Yang et al.  
16 2022). However, above results appear to contrast with the CMIP5 multimodel response, which  
17 suggests that the relatively smaller eruptions of Pinatubo size could trigger an El Niño-like  
18 response after about a year following the eruption peak (Maher et al. 2015; Fadnavis et al. 2021;  
19 Khodri et al. 2017). The 2011 Nabro eruption (erupted near the southern Red Sea region) was  
20 smaller than Pinatubo, however, it also produced an El Niño-like response that persisted for two  
21 years following the eruption that weakened the Indian summer monsoon and caused droughts  
22 (Fadnavis et al. 2021). Part of these differences are likely to be associated with differing model  
23 background states and biases, but may also be associated with experimental design (e.g., volcanic  
24 events ensemble members used in the composite). Consideration of water vapor feedback in the  
25 model during the simulation of eruption events could also play important role to account for such  
26 differences (Soden et al. 2002). The initial state (i.e., ocean preconditioning) of the Pacific has also  
27 proved to be very important (Predybaylo et al. 2017, 2020; Khodri et al. 2017). The dependence of  
28 ENSO's response to Pacific Ocean preconditioning for a Pinatubo-size eruption has been  
29 investigated by Predybaylo et al. (2017) using GFDL-CM2.1 coupled model, which reported that  
30 relative to an unperturbed simulation, an El Niño-like statistically significant warming appears for  
31 all ocean preconditioning states, except for a La Niña initial state introduced in the Pacific. A  
32 weaker El Niño condition happens following an El Niño initial state in the equatorial eastern Pacific  
33 (EP) compared to a central Pacific (CP) initial state. This suggests that initial states associated to  
34 different ENSO flavors (i.e., CP or EP ENSO) are also important as their global and regional  
35 impacts especially on the Hadley and walker circulations and associated impacts on monsoon  
36 system is largely different (Dogar et al. 2019; Taschetto et al., 2020; Ma et al., 2022). Predybaylo et

1 al. (2017) and Khodri et al. 2017 further suggested that Pinatubo-size volcanic events cause an El  
2 Niño-like warming pattern under all projected scenarios that tend to lengthen El Niño events,  
3 shorten La Niña events, and produce anomalous warming signal in the tropical central Pacific  
4 Ocean during neutral preconditioning. Predybaylo et al. (2017) also examined the effect of the  
5 season of the eruption, and reported a stronger El Niño-like response for eruptions occurring in the  
6 boreal summer compared to spring and winter eruptions. These findings suggest that more research  
7 is warranted to systematically disentangle the discrepancy between model results attributable to  
8 model differences and/or the experimental methods.

9 Numerous dynamical mechanisms have been identified in CGCM based idealized studies  
10 of volcanic effects to elucidate how the zonally symmetric volcanic forcing can interact on ENSO  
11 mode. In all cases, it is assumed that the Pacific basin Bjerknes feedback has been initiated  
12 (Bjerknes, 1969), following the initial projection on the ENSO mode, which helps to intensify the  
13 initial SST anomaly. The El Niño induced by the tropical volcanism in these models is related to  
14 several suggested mechanisms: the oceanic dynamic thermostat mechanism (Predybaylo et al. 2017;  
15 Ohba et al. 2013), the equatorward movement of the Intertropical Convergence Zone caused by  
16 decreased evaporation on cloudless subtropical regions (Haywood et al. 2013; Lim et al. 2016 ), the  
17 western land-ocean temperature anomaly induced by thermal contrast (Predybaylo et al. 2017), and  
18 the westerly response to the suppressed West African monsoon (WAM) and warm pool  
19 precipitation (Khodri et al. 2017; Chai et al. 2020). Two other factors may also influence the  
20 simulation of El Niño-like responses after tropical volcanic eruptions: the initial condition of the  
21 ocean (e.g. Menegoz et al. 2018) and the strength of the eruption. It is difficult to replicate an El  
22 Niño when the initial ocean condition is already in the El Niño peak phase before the eruption (Liu  
23 et al. 2018). Furthermore, the volcanic eruption must be strong enough to stimulate an El Niño  
24 (Emile-Geay et al. 2008; Lim et al. 2016). The details of these mechanisms that allow ENSO  
25 modulation by volcanic forcing (i.e., subtropical wind stress curl, dynamical thermostat, and land  
26 temperature changes) can be seen in McGregor et al. (2020) and Zhu et al. (2021).

27 Liu et al. (2018) performed a millennium volcanic sensitivity experiment using CESM  
28 model version 1 (CESM1) forced with volcanic reconstructions of Gao et al. (2008), for 1500 years  
29 (i.e., 501 to 2000 AD), to identify the ENSO response to tropical and extratropical eruptions. CESM  
30 has been used effectively to investigate volcano-ENSO linkages (Stevenson et al. 2017; Otto-  
31 Bliesner et al. 2016). A long control simulation (2000 years) was performed as a reference where all  
32 external forcings were fixed at the values of year 1850. Using this long control run, a forced  
33 volcanic simulation is carried out for the period of 501 to 2000 AD, keeping the external forcing at  
34 the same level as used in the control run except that the reconstruction of volcanic aerosols  
35 spanning 501 to 2000 AD was added as a variable driving force (Gao et al. 2008). During the  
36 simulated 1500 years, there were 25 tropical, 16 NH, and 13 SH volcanoes. In these sensitivity

1 experiments, it is noticed that, compared to the internal El Niño in the control run (Figure 6), the  
2 shift from El Niño to La Niña is quicker for the tropical volcanic-induced El Niño. The negative  
3 NINO3 index emerges early in May for this forced El Niño mode, which only appears in July for  
4 the internal mode in the control run. The La Niña following the El Niño for the volcanic-forced  
5 mode is also stronger than the purely internal ENSO. The easterly anomalous wind over the western  
6 Pacific appears in May after the El Niño for the internal mode, while it appears early in January and  
7 is stronger for the eruption forced mode. Since the volcanic forcing could be weak during this El  
8 Niño-La Niña transition time, which is the second year after the eruptions, this quick transition after  
9 the tropical volcanic-induced El Niño is a dynamically driven, oscillatory response to the preceding  
10 El Niño. These results resemble the results of Maher et al. (2015) who analyzed CMIP5 based  
11 models and showed a La Niña-like response couple years after the large tropical eruptions.

## 12 **5.2. Extratropical Volcanic Eruptions**

13 Much modeling work has been done on the impacts of tropical volcanism, especially their role in  
14 reducing monsoonal precipitation due to their strong impact on the ascending branch of Hadley Cell  
15 and associated equatorward shifting of the Intertropical Convergence Zone, as well as strong  
16 linkage to ENSO dynamics (Mass and Portman 1989; McCracken and Luther, 1984; Joseph and  
17 Zeng, 2011; Haywood et al. 2013; Dogar et al. 2017; Dogar and Sato 2019; Fadnavis et al. 2021).  
18 However, despite the strong sensitivity of ENSO variability to eruptions, very less model studies  
19 are conducted so far to examine the impacts of extratropical eruptions occurring in the Northern and  
20 Southern Hemispheres (i.e., NH and SH) (Stevenson et al. 2016, 2017; Liu et al. 2018; Zuo et al.  
21 2018; Pausata et al. 2015, 2016). Extratropical volcanic eruptions are less studied than tropical  
22 eruptions, since their radiative forcings were considered hemispheric only, as aerosols were  
23 confined to the eruption hemisphere rather than the global. Their hemispheric TOA radiative  
24 forcing can shift the Intertropical Convergence Zone (ITCZ) towards the warmer hemisphere  
25 (Haywood et al. 2013). This is consistent with earlier studies that have highlighted the potential  
26 regional impact of large extratropical eruptions on the amplitude of the Asian monsoons (Oman et  
27 al. 2005; Liu et al. 2022) and rainfall in Africa (Oman et al. 2006, Haywood et al 2013). Recent  
28 studies, however, have shown the possible global impacts of extratropical volcanism through their  
29 impacts on ENSO and/or oceanic circulation (e.g., Pausata et al. 2015, 2016; Stevenson et al. 2016;  
30 Liu et al. 2018; Zuo et al. 2018). Since, ocean integrates the volcanic signal and responds on a wide  
31 range of time scales (Stenchikov et al. 2009; Pausata et al. 2015; Dogar et al. 2020), therefore, the  
32 modulation of ocean circulation by extratropical eruptions allows their effects to last for decades.

33 For extratropical NH eruptions, models simulate a trend towards enhanced El Niño  
34 occurrence in the boreal winter after the eruption but differ on whether El Niño-like or La Niña-  
35 like states are expected in the second winter (Pausata et al. 2015; Zuo et al. 2018; Stevenson et al.

1 2016). An inclination towards a La Niña-like response was identified one year after an extratropical  
2 SH eruption (Stevenson et al. 2016), suggesting a rebound of El Niño-like conditions, as La Niña  
3 conditions normally follow El Niño states (Ohba & Ueda, 2009; Kessler, 2002; Okumura & Deser,  
4 2010). Additional modeling studies and research is needed to verify the proposed dynamic  
5 processes and to verify whether such influences of the initial conditions are sufficient to explain the  
6 completeness of this response. In the CESM model, the response to SH eruptions appear almost  
7 opposite to the response to NH eruptions during the year of eruption. Which is, the SH eruption  
8 events cause a northward ITCZ shift together with a strong initial cooling that peaks in the post-  
9 eruption boreal winter (Haywood et al. 2013; McGregor et al. 2020). However, the findings of  
10 Stevenson et al. (2016) suggest that this response is unlikely to have dynamics consistent with the  
11 La Niña episode based on the analysis of the complete spatial pattern of SST anomalies (Stevenson  
12 et al. 2016). A rebound to neutral ENSO conditions ensues, which roughly last for the next one  
13 year, during which further cooling occurs in the tropical Pacific.

14 The millennium volcanic sensitivity study by Liu et al. (2018) showed that after the NH eruptions  
15 (Figure 7a), the westerly wind anomalies are excited via the Bjerknes feedback to the south of the  
16 equator in the first northern winter over the Pacific, and warm SSTs initiate to develop from the  
17 eastern Pacific after the northern spring related with westerly wind anomalies. The warm SSTs also  
18 initiate to develop in the Eastern Pacific related with the equatorial westerly wind anomalies since  
19 the first northern winter after the tropical eruptions (Figure 7b). After SH eruptions, anticyclonic  
20 wind anomalies dominate in the Southeast Pacific (Figure 7c) associated with cold sea surface  
21 temperature anomalies. It has been shown that compared to westerly wind (and associated surface  
22 current) anomalies and their related descending in the central to eastern Pacific, one year after the  
23 NH or the tropical eruptions, the easterly wind (and surface current) anomalies and the associated  
24 ascending dominate the eastern Pacific one year after the SH eruptions (Figure 8). Thus, this  
25 ascending wind, via the Bjerknes feedback (Bjerknes, 1969), inhibits warm SST anomalies to  
26 develop in the eastern Pacific.

27  
28 One major mechanism has been identified that potentially contributes as an instant ENSO response  
29 to volcanic events occurring in extratropics, that lasts for about one year, is the shift of the ITCZ.  
30 Extratropical volcanic eruption events are characterized by the spread of sulfate aerosol, limited to  
31 the hemisphere in which the volcanic eruption occurs. It is commonly known that asymmetric  
32 interhemispheric forcing drives the ITCZ away from the hemisphere being cooled by volcanism  
33 (Kang et al. 2008; Dogar et al. 2017; Haywood et al. 2013; Schneider et al. 2014). This has been  
34 shown in coupled model studies of extratropical eruptions, for instance, simulations of the 1783  
35 Laki eruption in Iceland (Pausata et al. 2015) and entire millennium simulations of extratropical  
36 eruptions (Stevenson et al. 2017; Colose et al. 2016). The migration of the ITCZ towards the

1 equator, in response to a NH eruption, tends to favor the commencing of El Niño events (Pausata et  
2 al. 2015; Pausata et al. 2020) although more work is needed to accurately estimate the change in  
3 occurrence frequency. Since surface easterly winds are weakest in the immediate vicinity of the  
4 ITCZ, this migration to the equator implies a weakening of easterly winds along the equator in the  
5 central and eastern equatorial Pacific Ocean. Through the Bjerknes feedback mechanism (Bjerknes,  
6 1969), this weakening of the trade winds result in a decrease in the temperature contrast between  
7 east and west in the tropical Pacific, that favors the development of an El Niño–like anomaly. These  
8 El Niño–like anomalies could also be affected by the ocean preconditioning (see section 5 for  
9 details), that is, pre-existing or background ENSO state: a stronger El Niño–like response develops  
10 when the preexisting ocean state is La Niña rather than El Niño (Pausata et al. 2016).

11 The ITCZ’s potential role in inciting ENSO response in the first winter following the  
12 extratropical NH eruptions has also been proposed by Stevenson et al. (2016), who show the  
13 migration of the ITCZ to the equator after the eruption and subsequent development of El Niño-like  
14 conditions. In other earlier studies that examined the impacts of extratropical volcanic forcing on  
15 climate (Highwood & Stevenson, 2003; Haywood et al., 2013; Oman et al. 2005, 2006), an analysis  
16 of the ENSO response was not feasible due to the lacking of a fully coupled atmosphere-ocean  
17 model and the consequent failure to recognize coupled feedbacks. However, by using the coupled  
18 model simulations (fully coupled or coupled with a mixed oceanic layer), Zeng (2003), Oman et al.  
19 (2005, 2006), and Haywood et al. (2013) showed a suppressing of the Asian and/or African  
20 monsoon after the NH eruptions, suggesting a displacement of the ITCZ towards south that  
21 provides suitable conditions for the development of El Niño. The study by Zeng (2003), Dogar et al.  
22 (2019) further emphasize that the shift of ITCZ and subsequent weakening of monsoon is caused  
23 due to El Niño–like SST conditions, which could be related or unrelated to volcanism. This  
24 suggests that the ITCZ response to individual forcing (i.e., ENSO or volcanism) or their concurrent  
25 ENSO-volcano effect requires specifically designed coupled model sensitivity experiments for  
26 better understanding of volcano-ENSO-ITCZ linkage.

27

## 28 **6. Volcano-ENSO Linkage and AMOC Role**

29 The intense radiative cooling caused by large tropical volcanic eruptions and allied changes in  
30 atmospheric circulation result in colder, saltier and therefore denser upper ocean conditions over  
31 convective regions, causing modifications to the oceanic thermohaline circulation (e.g., Otterå et al.  
32 2010; Stenchikov et al. 2009; Raible et al. 2016; Dogar et al. 2020). This lets the cold signal to enter  
33 into the deep ocean and to substantially affect the global ocean temperature, sea level and heat  
34 content for several decades or even longer (Church et al. 2005; Delworth et al. 2005; Gleckler et al.  
35 2006; Fasullo et al. 2016), thereby protracting the recovery of the climate system from volcanic  
36 perturbations. A statistically significant Atlantic meridional overturning circulation (AMOC)



1 response after strong tropical volcanic eruption of Krakatau 1883 that persisted for several decades  
2 with associated northward enhancement in heat transport was reported in a study conducted using  
3 Met Office Unified Coupled Model, HadCM3 (Iwi et al. 2012). Similar to tropical volcanism,  
4 AMOC responds significantly to NH extratropical eruptions as well, predominantly due to a strong  
5 post-eruption ocean cooling that could last for few decades (e.g., Pausata et al. 2015). Numerous  
6 studies (both modeling and observational) proposed that AMOC forced changes could modulate the  
7 amplitude of ENSO (e.g., Dong & Sutton, 2002; Zhang & Delworth, 2005; Sutton et al. 2007;  
8 Timmermann et al. 2007; Pausata et al. 2015; Levine et al. 2017, 2018; Otto-Bliesner et al. 2016;  
9 Orihuela et al. 2022). Using a global climate model, Orihuela et al. (2022) showed that forced  
10 AMOC changes (i.e., slowdown or collapse under anthropogenic forcing) accelerates the Pacific  
11 trade winds and Walker circulation that results in enhanced subsidence and cooling over the east  
12 Pacific leading to a La Nina-like condition. The reverse is true for volcanic-induced changes in  
13 AMOC (i.e., strengthening under volcanism) that would result in warming over east Pacific that  
14 leading to an El Niño-like condition. This relationship is believed to be essentially due to large-  
15 scale changes in atmospheric circulation caused by AMOC-induced tropical Atlantic SST gradients,  
16 modulating the tropical Pacific, and ENSO (Ruprich-Robert et al. 2017; Polo et al. 2014; Dong et  
17 al. 2006; Orihuela et al. 2022). In addition, on a multi-decade scale, thermocline signals related with  
18 AMOC strength can also be transferred from the North Atlantic to the tropical Pacific via ocean  
19 waves (Timmermann et al. 2005). These modeled oceanic inter-basin relationships denoting that  
20 AMOC strong variability results in some variability in the ENSO could be physically reasonable  
21 (Atwood, 2015; Timmermann et al. 2007; Ding et al. 2014). However, there are limited  
22 observational data to support this oceanic inter-basin ENSO modulation (Atwood, 2015). With  
23 regard to extratropical eruptions, Pausata et al. (2015) examined the ENSO modulation following a  
24 volcanic event under modern conditions, and indicated that ENSO variance increases with an  
25 increase in AMOC and vice versa. The increased variability of ENSO during periods of strong  
26 AMOC is believed to be related to the flattening and shallowing of the thermocline in the equatorial  
27 Pacific, which enhances the Bjerknes feedback (Russell & Gnanadesikan, 2014; Pausata et al.  
28 2015). More research is needed to investigate the relationship between ENSO variability and  
29 AMOC after volcanic eruptions to better quantify long-term climate impacts beyond the lifespan of  
30 injected stratospheric aerosols.

### 31 **7. Role of Ocean Preconditioning, Eruption Location, Seasonality, and Magnitude.**

32 Two mechanisms, land-ocean temperature contrast (LOTC) and the oceanic dynamic  
33 thermostat (ODT) are largely proposed to explain volcano-ENSO linkage predominantly for low  
34 latitude tropical eruptions (e.g., Pokarel and Sikka, 2013; Gregory et al. 2016; Adam et al. 2003  
35 2016; Noh et al. 2017; Fadnavis et al. 2019; 2021). Both these mechanisms can activate westerly  
36 wind anomalies that consequently lead to El Niño-like SST response following strong volcanic

1 event. The LOTC is based on the heat capacity difference of the land and the ocean; the volcanic-  
2 induced temperature contrast between the western Pacific Ocean (WP) and the maritime continent  
3 is thought to weaken the trade winds. The ODT relies on the ability of ocean to moderate the SST  
4 response to radiative forcing more efficiently in the equatorial region of the eastern Pacific (EP),  
5 leading to temperature contrasts between the WP and the EP. Since the ODT is connected with the  
6 force of upwelling of equatorial ocean, its strength is closely related to preconditioning of ENSO  
7 (i.e., initial state) and, therefore, could also be the cause for divergent strength of the El Niño  
8 response following volcanic eruptions.

9 A study using the CESM climate model indicated another mechanism attributing to a  
10 stronger El Niño-like response following the tropical volcanism, associated with post-volcanic El  
11 Niño excitation via wind stress curl. This El Niño excitation appears due to post-eruption increased  
12 equatorial Pacific surface cooling and associated increased heat advection (Stevenson et al. 2017).  
13 Khodri et al. (2017) analyzed the CMIP5 simulations along with idealized experiments conducted  
14 using the Institute Pierre-Simon Laplace coupled climate model (with and without volcano) to  
15 understand the key mechanisms of ENSO-volcano linkage. This study linked an El Niño-like  
16 response to a volcanic-induced abrupt African continent, which lessened the West-African monsoon  
17 and produced westerly wind anomalies in the Western Pacific (Khodri et al. 2017; Fadnavis et al.  
18 2021). A study based on the Norwegian Earth System Model (NorESM) examined the ENSO  
19 response to asymmetrically distributed volcanic plume after the tropical volcanic eruptions (Pausata  
20 et al. 2016; Pausata et al. 2020). It emphasizes that the leading response mechanisms are related to  
21 extratropical circulation changes including shift of the Pacific jet and the changes in the cyclonic  
22 surface pressure anomalies in the Pacific mid-latitude region, while the shift of the ITCZ has a  
23 lesser role. Nevertheless, for high-latitude eruptions, it has been suggested that an explosive  
24 volcanic eruption occurring in the Northern Hemisphere (NH) shift the ITCZ equatorward and thus  
25 produce an El Niño-like response (Pausata et al. 2016). However, the variations between ENSO  
26 responses to massive volcanism and underlying mechanisms reported in these studies could stem  
27 from the inadequate sampling for temporal composites and ensembles. Hence, while investigating  
28 the ENSO response to volcanism, the sampling paradigm should essentially account for the  
29 following aspects:

30  
31 a. An ENSO onset (or ENSO preconditioning) that is connected with a set of atmospheric and  
32 oceanic conditions before the eruption (Predybaylo et al. 2017, 2020; Pausata et al. 2016; Marshall  
33 et al. 2022). These initial conditions are known as Neutral, El Niño, or La Niña starts (i.e., onsets),  
34 and in the nonexistence of external forcing, lead to corresponding neutral “normal”, negative, or  
35 positive ENSO years. The response of tropical Pacific relies strongly on ocean preconditioning  
36 irrespective of eruption type (i.e., high-latitude or low-latitude). For instance, Normal or El Niño

1 inceptions are more likely to be interfered by low-latitude eruptions than a La Niña onset  
2 (Preddybaylo et al. 2017, 2020; Ohba et al. 2013). Moreover, CP-type El Niño onsets may respond  
3 more intensely than EP-type El Niño onsets (Preddybaylo et al. 2017). For instance, global and  
4 regional impacts of different ENSOs (e.g., CP and EP-type) especially on the Hadley and Walker  
5 circulations and associated impacts on monsoon system are largely different (Dogar et al. 2019;  
6 Taschetto et al., 2020; Ma et al., 2022).

7

8 b. Timing of volcanic eruption related to the seasonal cycle or ENSO type (Stevenson et al. 2017;  
9 Preddybaylo et al. 2017; 2020) that may mask strong sensitivity of the ENSO response. Modeling  
10 studies show evidences that ENSO type and its response to volcanism is sensitive to the timing and  
11 seasonality of volcanic forcing. It is further found that the ENSO response is more robust in  
12 summer than in winter (Preddybaylo et al. 2017; 2020; Wittenberg et al. 2014), which could be  
13 explained by the widely known boreal spring (Feb-May) predictability barrier of ENSO event  
14 (McPhaden, 2003; Lai et al. 2018; Ren et al. 2018). This ENSO spring barrier suggests that the  
15 ENSO prediction skill is significantly reduced during the boreal spring, because of the tendency of  
16 the ENSO episode to shift towards El Niño and La Niña phases decay after their usual winter peak.  
17 It is noticed that the coupled climate models face problems in predicting boreal winter tropical  
18 Pacific SST when forecasts start in boreal spring (Lai et al. 2018; Zheng et al. 2010). Since volcanic  
19 eruptions can occur at any time of the year (Mason, 2004), it is therefore important to separately  
20 examine the impacts of volcanic eruptions occurring at different times.

21

22 c. Magnitude of volcanic activity that is responsible for ENSO response strength. The stronger the  
23 volcanic eruption, the more significant (or more likely) the ENSO response may be (Preddybaylo et al.  
24 al. 2017; 2020). For example, the Tambora eruption (three times larger than the Pinatubo), would  
25 cool the surface of the EP more within the first year, and then induce a warmer El Niño in the  
26 second year than a Pinatubo-sized eruption (Emile-Geay, 2008; Ohba et al. 2013; Stevenson et al.  
27 2017; Preddybaylo et al. 2017; McGregor et al. 2011; Li et al. 2013).

28

29 d. Location of the volcanic eruption, which is responsible for the aerosol plume distribution and  
30 lifetime. Though volcanic aerosols are normally globally distributed for most low-latitude  
31 eruptions, they may sometimes be trapped in one hemisphere (Pausata et al. 2020), and for high-  
32 latitude explosive eruptions are hemispherically distributed (Oman et al. 2005; Schneider et al.  
33 2009; Kravitz and Robock, 2011; Pausata et al. 2020). All these eruption types can cause a  
34 significant ENSO response (Liu et al. 2018). However, the sensitivity of ENSO response is less  
35 pronounced for high-latitude eruptions than for low-latitude eruption events due to relatively shorter

1 aerosol lifespan and varying interfering response mechanisms (Pausata et al. 2015, 2016; Sun et al.  
2 2019; Colose et al. 2016; Stevenson et al. 2016).

### 3 **8. Post-Volcanic Winter Warming and the Role of Internal Climate Variability**

4 Volcanic eruptions are believed to affect the Eurasian and North American winter temperatures  
5 (Shindell et al. 2004; Stenchikov et al. 2002; Schneider et al. 2009). In the first winter following the  
6 1991 eruption of Pinatubo, an increase in surface temperature reaching up to 3 °C was observed on  
7 the Eurasian continent, which was attributed to the recovery of global temperature following a  
8 volcanic eruption (e.g., Robock, 2002). While this 1991–1992 winter warming pattern could be  
9 considered to be triggered by natural climate variability (e.g., Polvani et al. 2019), Eurasian winter  
10 warming pattern was also seen in the first NH winter after three other tropical volcanic eruptions  
11 (Xing et al. 2020). This post-eruption European warming was also seen in 500-year multi-proxy  
12 reconstructions of 15 major tropical eruptions (Fischer et al. 2007). These responses are consistent  
13 with a forced volcanic response of the NAO. Some modeling studies have reported the cooling over  
14 the Middle East and North Africa after large eruptions, suggesting that it is part of a circulation  
15 response of same origin as the winter warming in Eurasia (Robock and Mao, 1992; Robock, 2002;  
16 Shindell et al. 2004; Osipov et al. 2016; Dogar et al. 2017; 2019; Dogar, 2020). However, there are  
17 only a few studies available that analyzed the underlying possible causes of the seasonal climate  
18 variability triggered by volcanic eruptions, that is winter warming over Eurasia and cooling patterns  
19 over Middle East and North Africa (MENA) respectively (e.g., Haywood et al. 2013; Dogar et al.  
20 2017), so the dynamic feedbacks processes and forced circulation changes still remain poorly  
21 understood. The Eurasian winter warming teleconnection is also potentially related to  
22 stratosphere–troposphere interaction. It has been shown that a tropical volcanic eruption can  
23 directly warm up the lower part of the tropical stratosphere since the aerosol clouds interact and  
24 absorb incoming near-infrared (NIR) and outgoing longwave radiation. Volcanic aerosols also  
25 deplete polar ozone by affecting ozone photochemistry in stratosphere. As solar radiation is  
26 absorbed by ozone in stratosphere, ozone depletion will lead to lower temperatures (Stenchikov et  
27 al. 2002) in the polar region. Resultant stratospheric warming at low-latitudes and polar cooling  
28 intensify the meridional temperature contrast over the NH, eventuating in a strengthened NH winter  
29 polar vortex (Figure 9a). This strengthened polar vortex, potentially warms Eurasia by entrapping  
30 tropospheric wave energy (Robock, 2000; Butler et al. 2014; Perlwitz and Graf, 1995; Raible et al.  
31 2016). Mostly the CMIP5 (e.g., Xing et al. 2020) as well as CMIP6 models (Liu et al. 2020, Figure  
32 9) can simulate this low-latitude stratospheric warming. The strengthened polar vortex, however, is  
33 weak in the models compared to the reanalysis (Marshall et al. 2009), posing a challenge for the  
34 current simulation of stratospheric teleconnection.

35 Current GCMs are able to reproduce the direct responses to large tropical eruptions  
36 (Trenberth and Dai, 2007; Iles and Hegerl, 2014; Stevenson et al. 2016; Liu et al. 2016), but they

1 still lacks in simulating the indirect responses caused by post-volcanic circulation changes, that  
2 could be related or unrelated to volcanism (Ding et al. 2014; Marshall et al. 2009; Driscoll et al.  
3 2012; Maher et al. 2015; Zambri et al. 2017; Wang et al. 2018; Xing et al. 2020; Polvani et al.  
4 2019).

5           There is emerging debate on the volcanic indirect effect caused by circulation changes  
6 that apparently produced warming effects in the first two winters following tropical eruptions over  
7 Eurasia and North America. Previous studies have linked this Eurasian and North American  
8 warming (up to 3°C) of 1982-1983 and 1991-1992 winters to the 1982 El Chichon and 1991  
9 Pinatubo eruptions (Robock and Mao, 1992; Xing et al. 2020). Using a 500-year multi-proxy  
10 reconstruction, Fischer et al. (2007) also showed this warming pattern that occurred following  
11 major tropical eruptions. This eruption–Eurasian-warming has been assumed to be due to post-  
12 eruption stratosphere–troposphere interaction that caused strengthening of the stratospheric polar  
13 vortex and associated positive phase of North Atlantic Oscillation (Stenchikov et al. 2002).  
14 However, recent studies have argued that such winter warming may simply be a result of internal  
15 variability (Polvani et al. 2019) caused by the positive phase of the Pacific North American pattern  
16 (PNA) favored by the ongoing positive ENSO events (El Niños) at the time of the eruptions  
17 (Fujiwara et al. 2020; Wunderlich and Mitchel, 2017). The El Niño events could also have favored  
18 a North Atlantic Oscillation response through stratospheric pathways (Marshall et al. 2009; Ineson  
19 and Scaife, 2009; King et al. 2018) and hence could explain the Eurasian warm winters following  
20 El Chichon and Pinatubo eruptions. However, other studies have demonstrated that large volcanic  
21 eruptions enhance the probability and strength of El Niño events (Pausata et al. 2015; 2020;  
22 Stevenson et al. 2016); hence, volcanic eruptions may still be the initial trigger for the warm winters  
23 at high latitudes. No study has hitherto investigated this chain of teleconnections. Moreover, the  
24 ENSO-NAO teleconnection itself still remains controversial. Moreover, the initial conditions of  
25 both the atmosphere (e.g., Quasi-biennial Oscillation (QBO) phase in the stratosphere) and the  
26 ocean (e.g. ENSO) at the time of the eruptions can further complicate the atmospheric circulation  
27 response to volcanic eruptions. For example, the studies of Zeng (2003), and Dogar et al. (2017,  
28 2019) assessed the ITCZ seasonal shift and subsequent weakening of monsoon following strong  
29 ENSO forcing and reported that ITCZ southward shift over the south Asian monsoon belt is caused  
30 due to El Niño–like SST conditions, which could be related or unrelated to volcanism. These  
31 studies strongly suggest that the ITCZ response to internal or external climate forcings (i.e., ENSO  
32 or volcanism respectively) or their concurrent effect through ENSO-volcano linkage requires  
33 specifically designed coupled model sensitivity experiments in addition to VolMIP for better  
34 understanding of ENSO-volcano linkage. Modeling studies also show a strong negative/positive  
35 NAO–like pattern over the Atlantic Ocean following strong El Niño/La Nina forcing (Dogar et al.  
36 2017, 2019). This NAO-like North Atlantic ENSO response may largely be caused by ENSO

1 teleconnections through stratospheric pathways (e.g. Ineson and Scaife 2009) or it could simply be  
2 an extension of the PNA-like pattern (e.g. Bulić and Kucharski 2012). This negative NAO pattern  
3 produces significant impact and induces warm and wet anomalies over Southern Europe extending  
4 to Middle East and North African region (Dogar et al. 2017, 2019). Since the origin of winter  
5 warming is elusive, therefore, further research is highly needed to disentangle the climatic response  
6 to volcanic eruptions and improve our understanding of tropical-to-extratropical teleconnections.  
7 For this purpose a set of experiments as shown in the schematic (Figure 10, panel A and B) is  
8 proposed. It involves ensemble experiments with and without volcanic forcing (initialized with  
9 different ENSO states to see the effect of ocean preconditioning) that could be used to disentangle  
10 volcanic direct and indirect circulation changes. Such idealized experimental setup will also help us  
11 to figure out the recent controversies whether post-volcanic Eurasian and North American warming  
12 is related or unrelated to volcanism (Polvani et al. 2019; Fujiwara et al. 2020).

### 13 **9. Summary and Discussion**

14 Study of volcanism is very important due to their direct radiative and indirect (through their impacts  
15 on large scale circulation changes, e.g., ENSO and NAO) climatic effects. A better understanding of  
16 volcanism and its impacts on ENSO could help in reliable prediction of the ENSO response to  
17 future eruptions, therefore accurate detail of volcano-ENSO linkage is highly needed to determine  
18 the actual magnitude of the climatic response controlled by these important forcing factors. Reliable  
19 observational data for the volcanic eruptions occurring in the satellite era is available, which  
20 provide sufficient details for robust model-based simulation of the volcanic-induced climate  
21 response. However, for volcanic eruption events of the past, details of stratospheric aerosol size  
22 distribution and eruption timing need to be reconstructed from climate proxy data (Sigl et al. 2015).  
23 Although much work has been done so far using PMIP3 and CMIP5 based protocols to improve the  
24 reconstructions of the past volcanic forcing (Toohey et al. 2016), clarity about the timing  
25 (Stevenson et al. 2017) and latitudinal position (Fasullo et al. 2019) of the volcanic event and its  
26 forcing properties is still elusive (Ding et al. 2014; Marshall et al. 2018; Gautier et al. 2019). Hence,  
27 to better understand the impact of volcanism on ENSO, it is necessary to have refined  
28 reconstructions of both the ENSO variability and volcanic forcing. We note that both the  
29 seasonality of the radiative effects of volcanism (e.g., Toohey et al. 2011) and seasonally varying  
30 strength of ENSO (e.g., Nicholls, 2008; Lai et al. 2018; Zheng et al. 2010) have the potential to  
31 modify the strength of the response of ENSO to volcanism, but these effects have not been explored  
32 in detail.

33 Despite some discrepancies, most of the past studies using paleoclimate proxy data show an  
34 El Niño-like warming in the eruption year (about 70 % of reconstruction data) when specified with  
35 consistent volcanic eruptions dates and none of the ENSO reconstructions show a significant La  
36 Niña-like response. However, some reconstructions (Table 1) that show a significant El Niño-like

1 conditions during eruption year also show significant La Niña-like cooling a few years before or  
2 after the volcanically driven El Niño-like SST warming (McGregor et al. 2020). This suggests that  
3 the La Nina response seen in observations, paleoclimate proxy records, and model simulations after  
4 initial El Niño could be a reflection of oscillatory nature of ENSO dynamics by which La Niña  
5 events generally follow El Niño events (Okumura & Deser, 2010; e.g. Ohba & Ueda, 2009). It  
6 further emphasize that at least a portion of such signal seen in reconstructions could be attributed to  
7 natural variability (Polvani et al. 2019; 2020) rather than to volcanic forcing and large ensemble  
8 experiments are still needed to quantify the relative roles of internal and forced response. This also  
9 suggests that volcanic effects could persist for more than one year beyond the eruption. Various  
10 paleoclimate studies are available so far to reconstruct ENSO relationship to volcanism and mostly  
11 they show varying results. For instance, Dee and Steiger, (2022) tested the volcanism-ENSO  
12 linkage in the past 2000 years long records of PHYDA product and noticed a weak tropical Pacific  
13 response following large tropical volcanism resembling to El Niño. Moreover, inconsistencies were  
14 noticed in magnitudes and spatial patterns between climate models and PHYDA regarding ENSO-  
15 volcano linkage.

16 We noticed an emerging consensus in CGCM based studies that investigated the impact of  
17 tropical volcanic forcing on ENSO, with the vast majority showing an El Niño-like warming in the  
18 year after a tropical eruption (McGregor et al. 2020). Despite the coherent responses, the CMIP5  
19 and CMIP6 model response is significantly weaker than the observational composite (Liu et al.  
20 2020; Xing et al. 2020). Nevertheless, some recent studies based on CMIP5 simulations showed  
21 significantly larger (by 40-49 %) eruption-induced cooling than observations (Chylek et al. 2020).  
22 This disparity could be either because of the extent of the response is inaccurately modeled, or due  
23 to the coincidental occurrence of eruptions and El Niño events and/or model poor response to this  
24 coincidental interaction and linkage to other possible concurrent natural variability signals (e.g.  
25 Nicholls, 1988; Schneider et al. 2009; Driscoll et al. 2012; Polvani et al. 2019). Disparities in model  
26 responses and their inconsistency with observations and proxy-based reconstruction could also be  
27 partly related to the input of volcanic ash, which is neglected so far. Recently, it has been suggested  
28 that the contribution of volcanic ash should be taken into account in volcanic simulations as it turns  
29 out to be a key factor, but has been completely neglected due to its short lifespan (Zhu et al. 2021).  
30 Ash-rich particles dominate the optical properties of the volcanic cloud for at least the first two  
31 months, and therefore the initial lifetime of sulfur-rich gases is determined by the absorption of  
32 sulfur dioxide onto the ash, instead of the reaction with OH as generally assumed. This study  
33 further shows that approximately 43% more removal of volcanic sulfur from the stratosphere occurs  
34 within 2 months due to heterogeneous sulfur dioxide chemistry on volcanic ash than without.

35 While most CGCMs show El Niño-like response, the exact dynamical causes of the  
36 response is still elusive. Several mechanisms (e.g., ocean dynamical thermostat, wind stress curl,

1 and ocean-land temperature changes) have been proposed that apparently explain the projection of  
2 volcanic radiative cooling onto the ENSO variability, and different models favor different  
3 mechanisms. Apparently, the inconsistency among models is attributed to differing model  
4 dynamics, difference in feedbacks processes (e.g., Soden et al. 2002) and parameterizations or  
5 differing experimental design. Thus, the modeled response appears to be the sum or balance of  
6 multiple feedback projections. Since the balance of feedbacks varies between models (e.g., Joshi  
7 and Shine, 2003; Lloyd et al. 2011; Soden et al. 2002), therefore, how ENSO reacts to volcanic  
8 forcing may also vary across models.

9 Compared to tropical eruptions, there are fewer studies available to date that investigated  
10 the impact of extratropical Northern/Southern Hemisphere (NH/SH) volcanic eruptions on ENSO  
11 (Schneider et al. 2009; Pausata et al. 2015, Stevenson et al. 2016; Liu et al. 2018; Zuo et al. 2018).  
12 These studies are consistent and show El Niño-like conditions emerging in the first year following  
13 NH eruptions (e.g., Stevenson et al. 2016; Pausata et al. 2015, 2016). Cold conditions in the  
14 equatorial Pacific are more likely to appear following SH eruptions, but this could not be similar to  
15 typical dynamical La Niña-like response (Stevenson et al. 2016; Pausata et al. 2020). ITCZ shift  
16 due to post-eruption cooling has been proposed as the leading mechanism for the ENSO response  
17 (Pausata et al. 2020; Stevenson et al. 2016), while the other mechanisms (the ocean dynamical  
18 thermostat, the cooling of tropical northern Africa or the Maritime continent) commonly invoked to  
19 explain the post-eruption ENSO response appear to be of secondary importance (e.g., Ward et al.  
20 2020; Pausata et al. 2020). A La Niña-like cooling signature following volcanic-induced El Niño-  
21 like pattern is also reported in response to extratropical volcanic forcing, which is in agreement with  
22 observations and model simulations (e.g., Okumura & Deser, 2010; Ohba & Ueda, 2009). These  
23 results suggest that extratropical volcanic forcing could potentially influence ENSO for few years  
24 beyond an eruption. In conjunction to this, some recent modeling studies have also analyzed the  
25 potential role of ocean circulation about volcano-ENSO linkage especially for high-latitude  
26 eruptions and reported that this volcanically driven ENSO variability persisting for several decades  
27 beyond the eruption could be attributed to volcanically forced changes in Atlantic Meridional  
28 Overturning Circulation and associated changes in ocean heat content and sea level rise (e.g.,  
29 Church et al. 2005; Stenchikov et al. 2009; Mignot et al., 2011; Pausata et al. 2015; 2020). The role  
30 of ocean circulation is very important in terms of ENSO variability and response to volcanism as  
31 ocean accumulates the signal of external forcing and responds at multiple time scales (e.g., Church  
32 et al. 2005; Stenchikov et al. 2009). As tropical volcanism also caused comparable perturbations in  
33 ocean circulation, especially in ocean heat content and sea level rise, (Church et al. 2005;  
34 Stenchikov et al. 2009; Mignot et al., 2011; Zanchettin et al. 2012; Dogar et al., 2020; Swingedouw  
35 et al. 2015), therefore one would anticipate predicting similar modulation of ENSO following  
36 tropical volcanism.



1 Our understanding of the evolution of ENSO and what ultimately leads to the occurrence of  
2 El Niño has improved considerably. Basically it is westerly wind anomalies over the western central  
3 equatorial Pacific that trigger Kelvin wave response leading to dynamically forced warming in the  
4 easternmost Pacific. It always starts with central Pacific warming, though (Graf 1986; Lai et al.  
5 2016, 2018; Fadnavis et al., 2021).

6 We noticed that the coupled model simulations show a southward (northward) shift of  
7 ITCZ following strong NH (SH) eruptions. Moreover, strong tropical eruptions (e.g., El Chichon  
8 and Pinatubo) also show a southward shift of ITCZ and associated weakening of South Asian  
9 monsoon in first two post-eruption summer seasons both in the observation analysis and high-  
10 resolution atmospheric model (HiRAM) simulations (Dogar and Sato, 2019). This ITCZ southward  
11 (northward) shift is also seen following strong El Niño (La Nina) conditions in AOGCM  
12 simulations with intermediate complexity (Dogar et al. 2017). This suggests that further systematic  
13 coupled model experiments are needed to better understand these interfering effects of ENSO and  
14 volcanism on the upward branch of Hadley Cell (i.e., ITCZ, e.g., Dogar, 2018). Similarly, varying  
15 mechanisms have been proposed regarding post-eruption high-latitude winter warming effect, such  
16 as this warming is argued to be caused by ENSO-induced NAO-like pattern or through volcanic-  
17 induced NAO-like pattern. This North Atlantic NAO-like ENSO response is also interpreted as an  
18 extension of the PNA pattern (e.g. Brönnimann et al. 2007; Bulić and Kucharski 2012), or it could  
19 simply be caused by ENSO teleconnections through a stratospheric pathways (e.g. Ineson and  
20 Scaife 2009). El Niño and La Nina events seem connected with extra-tropical climate anomalies  
21 through Pacific North American teleconnection pattern (Ropelewski and Halpert, 1986), therefore,  
22 it is of prime importance to understand the causes of interannual variability associated with ENSO  
23 and other climate phenomena (e.g., PNA and NAO) to fully understand the long-term effects of, for  
24 example, changes in volcanism on teleconnections (e.g., ENSO) and associated variations in global  
25 climate. Since the exact origin of post-eruption winter warming is still elusive, therefore, idealized  
26 experiments in addition to VolMIP as proposed in Figure 10 are needed to enhance our  
27 understanding on the complex ENSO-volcano linkage and associated climatic impacts.

28 A thorough assessment of the past literature shows that, in general, CMIP based models  
29 show agreement on the underlying mechanisms of El Niño-like response triggered by tropical  
30 eruptions, however, uncertainties still exist among modeled responses to volcanism happening in  
31 the tropics and extratropics. The causes of such disparities are still elusive, however, apparently  
32 these could be related to intermodal differences in experimental design, the quantity of ensemble  
33 members including methods used to construct the ensembles, model resolution, differing model top,  
34 input volcanic forcing data including its magnitude, seasonality, and the aerosol optical properties  
35 associated with sulfate injection (e.g., Stevenson et al. 2017; Toohey et al. 2011; Collins et al. 2010;  
36 McGregor & Timmermann, 2011; Zhu et al. 2021; Ohba et al. 2013). Moreover, model's limited

1 ability to simulate the contribution of internal variability related to large-scale circulation changes  
2 could add further to this uncertainty (Marshall et al. 2009; Driscoll et al. 2012; Zambri et al. 2017).  
3 Ocean precondition state (taking into account ENSO-types) at the time of eruption also adds to this  
4 ENSO-volcano complex linkage and intermodal inconsistency in projection of this nexus.  
5 Moreover, CP-type El Niño onsets may respond to volcanism more intensely than EP-type El Niño  
6 onsets. Response of Hadley and Walker circulations and associated regional monsoonal rainfall are  
7 also largely different for CP and EP-type ENSOs. This suggests the need for further studies on  
8 model sensitivity to radiative forcing with consistent experimental protocol and a large number of  
9 models and a large number of ensemble members. These idealized volcano-ENSO perturbation  
10 experiments designed to accurately account for the effect of natural variability (e.g., ENSO, PNA  
11 and NAO, Figure 10), in addition to the Model Intercomparison Project on the climate response to  
12 volcanic forcing, VolMIP (Zanchettin et al. 2016), will permit future research to emphasize on  
13 response differences that apparently originate from intermodal physical and dynamical differences.

#### 14 **10. Concluding Remarks**

15 Past literature based on short paleoclimate records and coupled model simulations suggest a  
16 significant eastern Pacific warming resembling an El Niño-like response during the eruption year  
17 and a lagged La Niña-like response few years after the eruption. However, long range climate  
18 reconstructions based on newly developed PHYDA product, spanning past 2000 years show a weak  
19 El Niño-like response of the tropical Pacific following volcanism. This is partly attributed to the  
20 statistical approaches employed to evaluate proxy based reconstructions as they seems sufficiently  
21 less sensitive in capturing ENSO response especially when there are strong chances of volcanic  
22 signal modulation with concurrent ENSO signal and the possibility of the interaction with internal  
23 variability caused by other large scale circulation changes (e.g., PNA and NAO). We further  
24 noticed that the ENSO response to volcanism is very sensitive to ocean preconditioning (especially  
25 different ENSO-types, i.e., EP and CP), eruption timing, position and magnitude. Moreover,  
26 stronger volcanic eruptions are expected to cause more significant ENSO response. We further  
27 noticed that some mechanisms of ENSO-volcano linkage still remain elusive. For example, how  
28 radiative cooling of tropical volcanism is projected onto ENSO contingent to the coincidental  
29 ENSO events unfolding at the time of the eruption. There are fewer observations and climate proxy  
30 records available to evaluate the effects of extratropical volcanism on ENSO. Nevertheless, model-  
31 based studies suggest that extratropical Northern (Southern) eruptions trigger a response similar to  
32 that of El Niño (La Niña). Emergence and significant amplification of El Niño-like conditions are  
33 also projected in a model simulation with RCP-8.5 future scenario following strong tropical  
34 eruptions of the size of Tambora 1815, and associated reduction in monsoonal rainfall (e.g., African  
35 and Asian-Australian monsoons) largely due to the post-volcanic land-ocean thermal contrast  
36 mechanism.

1 The specific cause of post-eruption winter warming is still elusive, however, recent findings  
2 suggest that the large-scale circulation changes concurrently occurring during volcanism could be  
3 the potential source of high-latitude winter warming over Eurasia and North America. We noticed  
4 that significant studies are available that highlight anthropogenic-driven ENSO changes and those  
5 derived by volcanism, however, combined interaction and ENSO response to both these external  
6 forcings (i.e., anthropogenic and volcanism) is not explored yet. Therefore, further research in this  
7 direction is recommended with consistent experimental protocol using multi-models and large  
8 ensembles accounting for the effects of internal variability and other large scale circulation changes,  
9 to explore the ENSO response to tropical and extratropical volcanism and to better understand  
10 whether post-eruption high-latitude winter warming is related or unrelated to volcanism.

### 11 12 13 **Acknowledgements**

14 The first author would like to thank the Japan Society for the Promotion of Science (JSPS) for  
15 providing a conducive environment and related resources to conduct this research under their  
16 postdoctoral fellowship research program in Japan. Additionally, comments and feedback from  
17 anonymous reviewers and Journal Editor are also acknowledged.

### 18 19 **Funding**

20 Part of this work is funded by Grant-in-Aid for JSPS Research Fellow.

### 21 **Declarations**

22 **Conflict of Interest**

23 The authors declare that there is no conflict of interest.

### 24 **References**

- 25 Adams, J. B., Mann, M. E., & Ammann, C. M. (2003). Proxy evidence for an El Niño-like response  
26 to volcanic forcing. *Nature*, 426(6964), 274–278. <https://doi.org/10.1038/nature02101>.
- 27 Anchukaitis, K. J., Buckley, B. M., Cook, E. R., Cook, B. I., D'Arrigo, R. D., & Ammann, C. M.  
28 (2010). Influence of volcanic eruptions on the climate of the Asian monsoon region. *Geophysical*  
29 *Research Letters*, 37(22). <https://doi.org/10.1029/2010GL044843>
- 30 Anchukaitis, K. J., Breitenmoser, P., Briffa, K. R., Buchwal, A., Büntgen, U., Cook, E. R., et al.  
31 (2012). Tree rings and volcanic cooling. *Nature Geoscience*, 5, 836. Retrieved from  
32 <https://doi.org/10.1038/ngeo1645>
- 33 Atwood, A. R. (2015). Mechanisms of tropical Pacific climate change during the Holocene.  
34 University of Washington.
- 35 Bader, J., Jungclauss, J., Krivova, N., Lorenz, S., Maycock, A., Raddatz, T., ... & Claussen, M.  
36 (2020). Global temperature modes shed light on the Holocene temperature conundrum. *Nature*  
37 *communications*, 11(1), 1-8.
- 38 Bellenger, H., Guilyardi, E., Leloup, J., Lengaigne, M., & Vialard, J. (2014). ENSO representation  
39 in climate models: From CMIP3 to CMIP5. *Climate Dynamics*, 42(7–8), 1999– 2018.  
40 <https://doi.org/10.1007/s00382-013-1783-z>

1 Bjercknes, J. (1969). Atmospheric teleconnections from the equatorial Pacific. *Monthly Weather*  
2 *Review*, 97(3), 163–172. [https://doi.org/10.1175/1520-0493\(1969\)097<0163:ATFTEP>2.3.CO;2](https://doi.org/10.1175/1520-0493(1969)097<0163:ATFTEP>2.3.CO;2)  
3 Bradley, R. S., & Jones, P. D. (1993) “Little Ice Age” summer temperature variations: Their nature  
4 and relevance to recent global warming trends. *Holocene*, 3, 367–376. doi:10.1177/  
5 095968369300300409  
6 Braganza, K., Gergis, J. L., Power, S. B., Risbey, J. S., & Fowler, A. M. (2009). A multiproxy  
7 index of the El Niño-Southern Oscillation, A.D. 1525-1982. *Journal of Geophysical Research*  
8 *Atmospheres*, 114(5), 1–17. <https://doi.org/10.1029/2008JD 010896>  
9 Briffa, K. R., Jones, P. D., Schweingruber, F. H., & Osborn, T. J. (1998). Influence of volcanic  
10 eruptions on Northern Hemisphere summer temperature over the past 600 years. *Nature*, 393, 450.  
11 Retrieved from <https://doi.org/10.1038/30943>  
12 Brönnimann S, Xoplaki E, Casty C, Pauling A and Luterbacher J 2007 ENSO influence on Europe  
13 during the last centuries, *Climate Dynamics*, 28(2-3), 181-197.  
14 Bulić I H, and Kucharski F 2012 Delayed ENSO impact on spring precipitation over North/Atlantic  
15 European region, *Climate dynamics*, 38(11-12), 2593-2612.  
16 Butler, A. H., L. M. Polvani, and C. Deser, 2014: Separating the stratospheric and tropospheric  
17 pathways of El Niño-Southern Oscillation teleconnections. *Environmental Research Letters*, 9,  
18 024014, <https://doi.org/10.1088/1748-9326/9/2/024014>.  
19 Cai, W., Santoso, A., Wang, G., Yeh, S. W., An, S. Il, Cobb, K. M., et al. (2015). ENSO and  
20 greenhouse warming. *Nature Climate Change*, 5(9), 849–859. <https://doi.org/10.1038/nclimate2743>  
21 Cai, W., Wang, G., Dewitte, B., Wu, L., Santoso, A., Takahashi, K., et al. (2018). Increased  
22 variability of eastern Pacific El Niño under greenhouse warming. *Nature*, 564(7735), 201–206.  
23 <https://doi.org/10.1038/s41586-018-0776-9>  
24 Chai, J., Liu, F., Xing, C., Wang, B., Gao, C., Liu, J., & Chen, D. (2020). A robust equatorial  
25 Pacific westerly response to tropical volcanism in multiple models. *Climate Dynamics*, 55(11),  
26 3413-3429.  
27 Christiansen, B. (2008). Volcanic Eruptions, Large-Scale Modes in the Northern Hemisphere, and  
28 the El Niño–Southern Oscillation. *Journal of Climate*, 21(5), 910–922. <https://doi.org/10.1175/2007JCLI1657.1>  
29 Church, J. A., White, N. J., & Arblaster, J. M. (2005). Significant decadal scale impact of volcanic  
30 eruptions on sea level and ocean heat content. *Nature*. <https://doi.org/10.1038/nature04237>.  
31 Chylek, P., Folland, C., Klett, J. D., & Dubey, M. K. (2020). CMIP5 Climate Models Overestimate  
32 Cooling by Volcanic Aerosols. *Geophysical Research Letters*, 47, e2020GL087047.  
33 <https://doi.org/10.1029/2020GL087047>.  
34 Clement, A. C., Seager, R., Cane, M. A., & Zebiak, S. E. (1996). An ocean dynamical thermostat, *J.*  
35 *Clim.*, 9, 2190–2196.  
36 Collins, M., An, S.-I., Cai, W., Ganachaud, A., Guilyardi, E., Jin, F.-F., et al. (2010). The impact of  
37 global warming on the tropical Pacific Ocean and El Niño. *Nature Geoscience*, 3(6), 391–397.  
38 <https://doi.org/10.1038/ngeo868>  
39 Colose, C. M., LeGrande, A. N., & Vuille, M. (2016). Hemispherically asymmetric volcanic  
40 forcing of tropical hydroclimate during the last millennium. *Earth System Dynamics*, 7(3), 681–  
41 696. <https://doi.org/10.5194/esd-7-681-2016>  
42 Cook, E. R. (2000). Niño 3 index reconstruction. In *International Tree-Ring Data Bank, IGBP*  
43 *PAGES/World Data Center for Paleoclimatology, Data Contribution Series #2000-052*. Boulder  
44 CO: NOAA/NGDC.  
45 Cook, E. R., D’Arrigo, R. D., & Anchukaitis, K. J. (2008). ENSO reconstructions from long tree  
46 ring chronologies: Unifying the differences? Presented at special workshop, “Reconciling ENSO  
47 Chronologies for the Past 500 Years,” Moorea, French Polynesia, 2–3 April 2008.  
48 Crowley, T. J., Zielinski, G. A., Vinther, B., Udisti, R., Kreutz, K., Cole-Dai, J., & Castellano, E.  
49 (2008). Volcanism and the Little Ice Age. *PAGES News*, 16(2), 22–23. <https://doi.org/10.1029/2002GL0166335>. Hegerl.

1 D'Arrigo, R., Wilson, R., & Jacoby, G. (2006). On the long-term context for late twentieth century  
2 warming. *Journal of Geophysical Research: Atmospheres*, 111(D3). <https://doi.org/10.1029/2005JD006352>  
3  
4 Dee, S.G., Cobb, K.M., Emile-Geay, J., Ault, T.R., Edwards, R.L., Cheng, H., Charles, C.D., 2020.  
5 No consistent ENSO response to volcanic forcing over the last millennium. *Science*, 367, 1477–  
6 1481. <https://doi.org/10.1126/science.aax2000>  
7 Dee, S. G., & Steiger, N. J. (2022). ENSO's Response to Volcanism in a Data Assimilation-Based  
8 Paleoclimate Reconstruction Over the Common Era. *Paleoceanography and Paleoclimatology*,  
9 37(3), e2021PA004290.  
10 Delworth, T. L., V. Ramaswamy, and G. L. Stenchikov (2005), The impact of aerosols on simulated  
11 ocean temperature and heat content in the 20th century, *Geophys. Res. Lett.*, 32, L24709.  
12 Ding, Y., Carton, J. A., Chepurin, G. A., Stenchikov, G., Robock, A., Sentman, L. T., & Krasting,  
13 J. P (2014). Ocean response to volcanic eruptions in Coupled Model Intercomparison Project 5  
14 simulations. *J. Geophys. Res. Oceans*, 119, 5622–5637. doi:10.1002/2013JC009780  
15 Dogar, M. M. (2018), Impact of tropical volcanic eruptions on Hadley circulation using a high-  
16 resolution AGCM, *Current Science* (00113891), 114(6).  
17 Dogar, M. M. A., & Almazroui, M. (2022). Revisiting the strong and weak ENSO teleconnection  
18 impacts using a high-resolution atmospheric model. *Atmospheric Environment*, 270, 118866.  
19 Dogar, M. M., Kucharski, F., Sato, T., Mehmood, S., Ali, S., Gong, Z., ... & Arraut, J. (2019).  
20 Towards understanding the global and regional climatic impacts of Modoki magnitude. *Global and*  
21 *planetary change*, 172, 223-241.  
22 Dogar, M. M., Kucharski, F., & Azharuddin, S. (2017). Study of the global and regional climatic  
23 impacts of ENSO magnitude using SPEEDY AGCM. *Journal of Earth System Science*, 126(2), 1-  
24 21.  
25 Dogar, M. M., G. Stenchikov, S. Osipov, B. Wyman, and M. Zhao (2017), Sensitivity of the  
26 regional climate in the Middle East and North Africa to volcanic perturbations, *Journal of*  
27 *Geophysical Research: Atmospheres*, 122, 7922-7948.  
28 Dogar, M. M., & Sato, T. (2019). Regional climate response of Middle Eastern, African, and South  
29 Asian monsoon regions to explosive volcanism and ENSO forcing. *Journal of Geophysical*  
30 *Research: Atmospheres*, 124(14), 7580-7598.  
31 Dogar, M., & Stenchikov, G. L. (2013, December). Study of Ocean Response to Periodic and  
32 Constant Volcanic Radiative Forcing. In *AGU Fall Meeting Abstracts* (Vol. 2013, pp. GC11C-  
33 0999).  
34 Dogar, M. M., Sato, T., & Liu, F. (2020). ocean Sensitivity to periodic and constant Volcanism.  
35 *Scientific reports*, 10(1), 1-15.  
36 Dogar, M. M. A. (2020). Study of the regional climatic impacts of tropical explosive volcanism in  
37 the Middle East and North Africa region (Doctoral dissertation, 北海道大学).  
38 Dogar, M. M. A., & Shahid, A. (2020, February). The Sensitivity of Ocean Temperature, Heat  
39 Content, Sea-Level Rise, and Atlantic Meridional Overturning Circulation to Periodic and Constant  
40 Volcanic Forcing. In *Ocean Sciences Meeting 2020*. AGU.  
41 Dong, B.-W., & Sutton, R. T. (2002). Adjustment of the coupled ocean-atmosphere system to a  
42 sudden change in the Thermohaline Circulation. *Geophysical Research Letters*, 29(15), 18-1-18-4.  
43 <https://doi.org/10.1029/2002GL015229>  
44 Dong B., R.T. Sutton and A.A. Scaife 2006. Multidecadal Modulation of El Niño-Southern  
45 Oscillation (ENSO) variance by Atlantic Ocean sea surface temperatures. *Geophys. Res. Lett.*, 33,  
46 L08705.  
47 Driscoll, S., Bozzo, A., Gray, L. J., Robock, A., & Stenchikov, G. L. (2012). Coupled Model  
48 Intercomparison Project 5 (CMIP5) simulations of climate following volcanic eruptions. *Journal of*  
49 *Geophysical Research Atmospheres*, 117(17), n/a-n/a. <https://doi.org/10.1029/2012JD017607>

1 Eddebbar, Y. A., Rodgers, K. B., Long, M. C., Subramanian, A. C., Xie, S.-P., & Keeling, R. F.  
2 (2019). El Niño–Like Physical and Biogeochemical Ocean Response to Tropical Eruptions. *Journal*  
3 *of Climate*, 32(9), 2627–2649. <https://doi.org/10.1175/JCLI-D-18-0458.1>

4 Emile-Geay, J., Seager, R., Cane, M. A., Cook, E. R., & Haug, G. H. (2008). Volcanoes and  
5 ENSO over the past millennium. *Journal of Climate*, 21(13), 3134–3148. <https://doi.org/10.1175/2007JCLI1884.1>

6 Emile-Geay, J., Cobb, K. M., Mann, M. E., & Wittenberg, A. T. (2013a). Estimating central  
7 equatorial Pacific SST variability over the past millennium. Part I: Methodology and validation.  
8 *Journal of Climate*, 26(7), 2302–2328. <https://doi.org/10.1175/JCLI-D-11-00510.1>

9 Emile-Geay, J., Cobb, K. M., Mann, M. E., & Wittenberg, A. T. (2013b). Estimating central  
10 equatorial Pacific SST variability over the past millennium. Part II: Reconstructions and  
11 implications. *Journal of Climate*, 26(7), 2329–2352. <https://doi.org/10.1175/JCLI-D-11-00511.1>

12 Evans, M. N., Cane, M. A., Schrag, D. P., Kaplan, A., Linsley, B. K., Villalba, R., & Wellington, G.  
13 M. (2001). Support for tropically driven Pacific decadal variability based on paleoproxy evidence.  
14 *Geophys. Res. Lett*, 28(19), 3689–3692.

15 Evans, M. N., Kaplan, A., & Cane, M. A. (2002). Pacific sea surface temperature field  
16 reconstruction from coral  $\delta^{18}\text{O}$  data using reduced space objective analysis. *Paleoceanography*,  
17 17(1), 1007. <https://doi.org/10.1029/2000PA000590>

18 Fadnavis, S., Sabin, T. P., Roy, C., Rowlinson, M., Rap, A., Vernier, J. P., & Sioris, C. E. (2019).  
19 Elevated aerosol layer over South Asia worsens the Indian droughts. *Scientific reports*, 9(1), 1-11.

20 Fadnavis, S., Müller, R., Chakraborty, T., Sabin, T. P., Laakso, A., Rap, A., ... & Tilmes, S. (2021).  
21 The role of tropical volcanic eruptions in exacerbating Indian droughts. *Scientific reports*, 11(1), 1-  
22 13.

23 Fasullo, J. T., Tomas, R., Stevenson, S., Otto-Bliesner, B., Brady, E., & Wahl, E. (2017). The  
24 amplifying influence of increased ocean stratification on a future year without a summer. *Nature*  
25 *Communications*, 8(1). <https://doi.org/10.1038/s41467-017-01302-z>

26 Fasullo, J. T., Otto-Bliesner, B. L., & Stevenson, S. (2019). The influence of volcanic aerosol meridional  
27 structure on monsoon responses over the last millennium. *Geophysical Research Letters*, 46(21), 12350-  
28 12359.

29 Fischer, E. M., Luterbacher, J., Zorita, E., Tett, S. F. B., Casty, C., & Wanner, H. (2007). European  
30 climate response to tropical volcanic eruptions over the last half millennium. *Geophysical Research*  
31 *Letters*, 34(5). <https://doi.org/10.1029/2006GL027992>

32 Folland, C.K., Boucher, O., Colman, A. and Parker D.E. (2018). Causes of irregularities in trends of  
33 global mean surface temperature since the late 19th century. *Sci. Adv.*, 4, eaao5297, DOI:  
34 10.1126/sciadv.aao5297.

35 Fujiwara, M., Hibino, T., Mehta, S. K., Gray, L., Mitchell, D., & Anstey, J. (2015). Global  
36 temperature response to the major volcanic eruptions in multiple reanalysis data sets. *Atmospheric*  
37 *chemistry and physics*, 15(23), 13507-13518.

38 Fujiwara, M., Martineau, P., & Wright, J. S. (2020). Surface temperature response to the major  
39 volcanic eruptions in multiple reanalysis data sets. *Atmospheric Chemistry and Physics*, 20(1), 345-  
40 374.

41 Fyfe, J. C., Gillett, N. P., & Zwiers, F. W. (2013). Overestimated global warming over the past 20  
42 years. *Nature Climate Change*, 3(9), 767–769. <https://doi.org/10.1038/nclimate1972>

43 Gao, C., Robock, A., & Ammann, C. (2008). Volcanic forcing of climate over the past 1500 years:  
44 An improved ice core-based index for climate models. *Journal of Geophysical Research*  
45 *Atmospheres*, 113(23), 1–15. <https://doi.org/10.1029/2008JD010239>

46 Gautier, E., J. Savarino, J. Hoek, J. Erbland, N. Caillon, S. Hattori, N. Yoshida, E. Albalat, F.  
47 Albarede, and J. Farquhar. "2600-years of stratospheric volcanism through sulfate isotopes." *Nature*  
48 *communications* 10, no. 1 (2019): 1-7.

49 Genin, A., B. Lazar, and S. Brenner (1995), Vertical mixing and coral death in the Red Sea  
50 following the eruption of Mount Pinatubo, *Nature*, 377(6549), 507.

51 Gill, A. E. (1980). Some simple solutions for heat induced tropical circulation. *Quarterly Journal of*  
52 *the Royal Meteorological Society*, 106(449), 447–462. <https://doi.org/10.1002/qj.49710644905>

53

1 Gleckler, P. J., Wigley, T. M. L., Santer, B. D., Gregory, J. M., AchutaRao, K., & Taylor, K. E.  
2 (2006). Krakatoa's signature persists in the ocean. *Nature*, 439(7077), 675-675.

3 Graf, H.-F., 1986: On the El-Niño/Southern Oscillation and Northern Hemispheric  
4 temperature. *Gerlands Beitr. Geo-phys.*, 95, 63-75.

5 Guilyardi, E., Bellenger, H., Collins, M., Ferrett, S., Cai, W., & Wittenberg, A. (2012). A first look  
6 at ENSO in CMIP5. *Clivar Exchanges*, 17(58), 29-32. Retrieved from  
7 [http://www.uib.no/People/ngfhd/EarthClim/Publications/Papers/Guilyardi\\_etal\\_2012.pdf](http://www.uib.no/People/ngfhd/EarthClim/Publications/Papers/Guilyardi_etal_2012.pdf)

8 Handler, P. (1984). Possible association of stratospheric aerosols and El Niño type events.  
9 *Geophysical Research Letters*, 11, 1121-1124. <https://doi.org/10.1029/GL011i011p01121>

10 Handler, P. (1986). Possible association between the climatic effects of stratospheric aerosols and  
11 sea surface temperatures in the eastern tropical Pacific Ocean. *Journal of climatology*, 6(1), 31-41.

12 Handler, P., & Andsager, K. (1994). El Niño, volcanism, and global climate. *Human Ecology*,  
13 22(1), 37-57.

14 Harshvardhan. (1979). Perturbation of the zonal radiation balance by a stratospheric aerosol layer.  
15 *Journal of the Atmospheric Sciences*. [https://doi.org/10.1175/1520-0469\(1979\)036<1274:POTZRB>2.0.CO;2](https://doi.org/10.1175/1520-0469(1979)036<1274:POTZRB>2.0.CO;2)

16 Haywood, J. M., A. Jones, N. Bellouin, and D. and Stephenson (2013), Asymmetric forcing from  
17 stratospheric aerosols impacts Sahelian rainfall, *Nature Climate Change*, 3, 660-665,  
18 doi:10.1038/nclimate1857.

19 Haywood, J. M., Jones, A., & Jones, G. S. (2014). The impact of volcanic eruptions in the period  
20 2000-2013 on global mean temperature trends evaluated in the HadGEM2-ES climate model.  
21 *Atmospheric Science Letters*, 15, 92-96. <https://doi.org/10.1002/asl2.471>

22 Hermanson, L., R. Bilbao, N. Dunstone, M. Menegoz, P. Ortega, H. Pohlmann, J.I. Robson, D.M.  
23 Smith, G. Strand, C. Timmreck, S. Yeager, and G. Danabasoglu (2020). Robust multi-year climate  
24 impacts of volcanic eruptions in decadal prediction systems, *JGR-A*, 125, e2019JD031739.

25 Hernández, A. et al (2020). Modes of climate variability: Synthesis and review of proxy-based  
26 reconstructions through the Holocene. *Earth-Science Reviews*, 209, 2020, 103286,

27 Highwood, E.-J., & Stevenson, D. S. (2003). Atmospheric impact of the 1783-1784 Laki Eruption:  
28 Part II. Climatic effect of sulphate aerosol. *Atmospheric Chemistry and Physics*, 3(4), 1177-1189.  
29 <https://doi.org/10.5194/acp-3-1177-2003>

30 Huang, B., Thorne, P. W., et al. (2017). Extended Reconstructed Sea Surface Temperature version 5  
31 (ERSSTv5): Upgrades, validations, and intercomparisons. *J. Climate*. doi: 10.1175/JCLI-D-16-  
32 0836.1

33 Iles, C. E., and G. C. Hegerl, 2014: The global precipitation response to volcanic eruptions in the  
34 CMIP5 models. *Environmental Research Letters*, 9, 104012, <https://doi.org/10.1088/1748-9326/9/10/104012>.

35 Ineson, S., and A. Scaife (2009), The role of the stratosphere in the European climate response to El  
36 Niño, *Nature Geoscience*, 2(1), 32-36.

37 Iwi, A. M., Hermanson, L., Haines, K., & Sutton, R. T. (2012). Mechanisms linking volcanic  
38 aerosols to the Atlantic meridional overturning circulation. *Journal of Climate*, 25(8), 3039-3051.

39 Jones, A. C., Haywood, J. M., Jones, A., and Aquila, V. (2016). Sensitivity of volcanic aerosol  
40 dispersion to meteorological conditions: A Pinatubo case study, *J. Geophys. Res. Atmos.*, 121,  
41 6892- 6908, doi:10.1002/2016JD025001.

42 Joshi, M. M., and K. P. Shine (2003). A GCM study of volcanic eruptions as a cause of increased  
43 stratospheric water vapour. *J. Clim.*, 16, 3525-3534.

44 Kang, S. M., Held, I. M., Frierson, D. M. W., & Zhao, M. (2008). The response of the ITCZ to  
45 extratropical thermal forcing: Idealized slab-ocean experiments with a GCM. *Journal of Climate*,  
46 21(14), 3521-3532. <https://doi.org/10.1175/2007JCLI2146.1>

47 Kessler, W. S. (2002). Is ENSO a cycle or a series of events? *Geophysical Research Letters*, 29(23),  
48 40-1-40-4. <https://doi.org/10.1029/2002GL015924>

49  
50

1 Khodri, M., Izumo, T., Vialard, J., Janicot, S., Cassou, C., Lengaigne, M., et al. (2017). Tropical  
2 explosive volcanic eruptions can trigger El Niño by cooling tropical Africa. *Nature*  
3 *Communications*, 8(1), 1–13. <https://doi.org/10.1038/s41467-017-00755-6>  
4 Kodera, K. (1994). Influence of volcanic eruptions on the troposphere through stratospheric  
5 dynamical processes in the northern hemisphere winter. *Journal of Geophysical Research:*  
6 *Atmospheres*, 99(D1), 1273–1282. <https://doi.org/10.1029/93JD02731>  
7 Kravitz, B., & Robock, A. (2011). Climate effects of high-latitude volcanic eruptions: Role of the  
8 time of year. *Journal of Geophysical Research: Atmospheres*, 116(D1). <https://doi.org/10.1029/2010JD014448>  
9  
10 Labitzke, K. and H. Van Loon (1989). The Southern Oscillation: Part IX: The influence of Volcanic  
11 Eruptions on the Southern Oscillation in the Stratosphere. *J. Clim.*, 21223-1226.  
12 Lai, A. W. C., Herzog, M., & Graf, H. F. (2015). Two key parameters for the El Niño continuum:  
13 zonal wind anomalies and Western Pacific subsurface potential temperature. *Climate Dynamics*,  
14 45(11), 3461-3480.  
15 Lai, A. W. C., Herzog, M., & Graf, H. F. (2018). ENSO forecasts near the spring predictability  
16 barrier and possible reasons for the recently reduced predictability. *Journal of Climate*, 31(2), 815-  
17 838.  
18 Levine, A. F. Z., McPhaden, M. J., & Frierson, D. M. W. (2017). The impact of the AMO on  
19 multidecadal ENSO variability. *Geophysical Research Letters*, 44(8), 3877–3886. <https://doi.org/10.1002/2017GL072524>  
20  
21 Levine, A. F. Z., Frierson, D. M. W., & McPhaden, M. J. (2018). AMO forcing of multidecadal  
22 Pacific ITCZ variability. *Journal of Climate*, 31(14), 5749–5764. [https://doi.org/10.1175/JCLI-D-](https://doi.org/10.1175/JCLI-D-17-0810.1)  
23 17-0810.1  
24 Li, J., Xie, S. P., Cook, E. R., Huang, G., D’arrigo, R., Liu, F., et al. (2011). Interdecadal  
25 modulation of El Niño amplitude during the past millennium. *Nature Climate Change*, 1(2), 114–  
26 118. <https://doi.org/10.1038/nclimate1086>  
27 Li, J., Xie, S. P., Cook, E. R., Morales, M. S., Christie, D. A., Johnson, N. C., et al. (2013). El Niño  
28 modulations over the past seven centuries. *Nature Climate Change*, 3(9), 822–826.  
29 <https://doi.org/10.1038/nclimate1936>  
30 Lim, H.-G., Yeh, S.-W., Kug, J.-S., Park, Y.-G., Park, J.-H., Park, R., & Song, C.-K. (2016).  
31 Threshold of the volcanic forcing that leads the El Niño-like warming in the last millennium:  
32 Results from the ERIK simulation. *Climate Dynamics*, 46(11), 3725–3736. <https://doi.org/10.1007/s00382-015-2799-3>  
33  
34 Liu, F., J. Chai, B. Wang, J. Liu, X. Zhang, and Z. Y. Wang, 2016: Global monsoon precipitation  
35 responses to large volcanic eruptions. *Scientific Reports*, 6, 24331,  
36 <https://doi.org/10.1038/srep24331>.  
37 Liu, F., Li, J., Wang, B., Liu, J., Li, T., Huang, G., & Wang, Z. (2018). Divergent El Niño  
38 responses to volcanic eruptions at different latitudes over the past millennium. *Climate Dynamics*,  
39 50(9–10), 3799–3812. <https://doi.org/10.1007/s00382-017-3846-z>  
40 Liu, F., Xing, C., Li, J., Wang, B., Chai, J., Gao, C., ... & Chen, D. (2020). Could the recent Taal  
41 volcano eruption trigger an El Niño and lead to Eurasian warming?  
42 Liu, F., Gao, C., Chai, J., Robock, A., Wang, B., Li, J., ... & Dong, W. (2022). Tropical volcanism  
43 enhanced the East Asian summer monsoon during the last millennium. *Nature communications*,  
44 13(1), 1-7.  
45 Lloyd, J., Guilyardi, E., & Weller, H. (2011). The role of atmosphere feedbacks during ENSO in the  
46 CMIP3 models. Part II: using AMIP runs to understand the heat flux feedback mechanisms.  
47 *Climate Dynamics*, 37(7), 1271–1292. <https://doi.org/10.1007/s00382-010-0895-y>  
48 Luo, J.-J., Liu, G., Hendon, H., Alves, O., & Yamagata, T. (2017). Inter-basin sources for two-year  
49 predictability of the multi-year La Niña event in 2010–2012. *Scientific Reports*, 7(1), 2276.  
50 <https://doi.org/10.1038/s41598-017-01479-9>  
51 Luther, F. M. (1976). Relative influence of stratospheric aerosols on solar and longwave radiative  
52 fluxes for a tropical atmosphere. *Journal of Applied Meteorology and Climatology*, 15(9), 951-955.



- 1 Ma, Y., Sun, J., Dong, T. et al. More profound impact of CP ENSO on Australian spring rainfall in  
2 recent decades. *Clim Dyn* (2022).
- 3 Maher, N., McGregor, S., England, M. H., & Gupta, A. S. (2015). Effects of volcanism on tropical  
4 variability. *Geophysical Research Letters*, 42(14). <https://doi.org/10.1002/2015GL064751>
- 5 Mann, M. E., Bradley, R. S., & Hughes, M. K. (2000). Long-term variability in the El Niño  
6 Southern Oscillation and associated teleconnections. In Diaz, H. F., & Markgraf, V. (Eds.), *El Niño*  
7 *and the Southern Oscillation: Multiscale variability and its impacts on natural ecosystems and*  
8 *society* (Vol. 2, pp. 321–372). Cambridge University Press.
- 9 Mann, M. E., Cane, M. A., Zebiak, S. E., & Clement, A. (2005). Volcanic and solar forcing of the  
10 tropical Pacific over the past 1000 years. *Journal of Climate*, 18(3), 447–456. <https://doi.org/10.1175/JCLI-3276.1>
- 11  
12 Mann, M. E., Fuentes, J. D., & Rutherford, S. (2012). Underestimation of volcanic cooling in tree-  
13 ring-based reconstructions of hemispheric temperatures. *Nature Geoscience*, 5, 202. Retrieved from  
14 <https://doi.org/10.1038/ngeo1394>
- 15 Marshall, L., Schmidt, A., Toohey, M., Carslaw, K. S., Mann, G. W., Sigl, M., et al. (2018). Multi-  
16 model comparison of the volcanic sulfate deposition from the 1815 eruption of Mt. Tambora. *Atmospheric Chemistry and Physics*, 18(3), 2307–2328. <https://doi.org/10.5194/acp-18-2307-2018>
- 17  
18 Marshall, L. R., Schmidt, A., Johnson, J. S., Mann, G. W., Lee, L. A., Rigby, R., & Carslaw, K. S.  
19 (2021). Unknown eruption source parameters cause large uncertainty in historical volcanic radiative  
20 forcing reconstructions. *Journal of Geophysical Research: Atmospheres*, 126(13), e2020JD033578.
- 21  
22 Marshall, L. R., Maters, E. C., Schmidt, A., Timmreck, C., Robock, A., & Toohey, M. (2022).  
23 Volcanic effects on climate: recent advances and future avenues. *Bulletin of Volcanology*, 84(5), 1-  
24 14.
- 25  
26 Marshall A., A.A. Scaife and S. Ineson (2009). Enhanced Seasonal Prediction of European Winter  
27 Warming following Volcanic Eruptions. *J. Clim.*, 22, 6168-6180.
- 28  
29 Mass, C. F., & Portman, D. A. (1989). Major volcanic eruptions and climate: A critical evaluation.  
30 *Journal of Climate*, 2(6), 566-593.
- 31  
32 McCracken, M., and F. Luther (1984), Preliminary estimate of the radiative and climatic effects of  
33 the El Chichón eruption, *Geofis. Int.*, 23-3, 385–401.
- 34  
35 Matsuno, T. (1966). Quasi-geostrophic motions in the equatorial area. *J Meteor Soc Jpn*, 44, 25–43.
- 36  
37 McGregor, S., Khodri, M., Maher, N., Ohba, M., Pausata, F. S., & Stevenson, S. (2020). The effect  
38 of strong volcanic eruptions on ENSO. *El Niño Southern Oscillation in a changing climate*, 267-  
39 287.
- 40  
41 McPhaden, M. J., Zebiak, S. E., & Glantz, M. H. (2006). ENSO as an integrating concept in earth  
42 science. *science*, 314(5806), 1740-1745.
- 43  
44 Medhaug, I., Stolpe, M. B., Fischer, E. M., & Knutti, R. (2017). Reconciling controversies about  
45 the ‘global warming hiatus.’ *Nature*, 545, 41. Retrieved from <http://dx.doi.org/10.1038/nature22315>
- 46  
47 Meehl, G.A., H. Teng, N. Maher, and M.H. England, (2015), Effects of the Mt. Pinatubo eruption  
48 on decadal climate prediction skill. *Geophys. Res. Lett.*, 42, 10,840-10,846,  
49 [doi:10.1002/2015GL066608](https://doi.org/10.1002/2015GL066608).
- 50  
51 Meinen, C. S., & McPhaden, M. J. (2000). Observations of warm water volume changes in the  
52 equatorial Pacific and their relationship to El Niño and La Niña. *Journal of Climate*, 13(20), 3551–  
53 3559. [https://doi.org/10.1175/1520-0442\(2000\)013<3551:OOWWVC>2.0.CO;2](https://doi.org/10.1175/1520-0442(2000)013<3551:OOWWVC>2.0.CO;2)
- 54  
55 Ménégoz et al. (2018). Forecasting the climate response to volcanic eruptions: prediction skill  
56 related to stratospheric aerosol forcing. *Environ. Res. Lett.* 13 064022.
- 57  
58 Mills, M. J., Schmidt, A., Easter, R., Solomon, S., Kinnison, D. E., Ghan, S. J., ... & Gettelman, A.  
59 (2016). Global volcanic aerosol properties derived from emissions, 1990–2014, using CESM1  
60 (WACCM). *Journal of Geophysical Research: Atmospheres*, 121(5), 2332-2348.
- 61  
62 Mignot, J., Khodri, M., Frankignoul, C., & Servonnat, J. (2011). Volcanic impact on the Atlantic  
63 Ocean over the last millennium. *Climate of the Past*, 7(4), 1439-1455.
- 64  
65 Mills, M. J., Richter, J. H., Tilmes, S., Kravitz, B., MacMartin, D. G., Glanville, A. A., ... &  
66 Kinnison, D. E. (2017). Radiative and chemical response to interactive stratospheric sulfate aerosols

1 in fully coupled CESM1 (WACCM). *Journal of Geophysical Research: Atmospheres*, 122(23), 13-  
2 061.

3 Monerie P.A., Moine M.-P., Terray L. and Valcke S. (2017). Quantifying the impact of early 21st  
4 century volcanic eruptions on global-mean surface temperature. *Environ. Res. Lett.*, 12, 054010.

5 Morice, C. P., Kennedy, J. J., Rayner, N. A., & Jones, P. D. (2012). Quantifying uncertainties in  
6 global and regional temperature change using an ensemble of observational estimates: The  
7 HadCRUT4 dataset. *Journal of Geophysical Research*, 117, D08101. doi:10.1029/2011JD017187

8 Nicholls, N. (1988). Low latitude volcanic eruptions and the El Niño-Southern Oscillation. *Journal*  
9 *of Climatology*, 8(1), 91– 95. <https://doi.org/10.1002/joc.3370080109>

10 Nicholls, N. (2008). Recent trends in the seasonal and temporal behaviour of the El Niño–Southern  
11 Oscillation. *Geophysical Research Letters*, 35(19). <https://doi.org/10.1029/2008GL034499>

12 Niemeier, U., Schmidt, H., & Timmreck, C. (2010). The dependency of geoengineered sulfate  
13 aerosol on the emission strategy. *Atmospheric Science Letters*, 12(2), 189–194. <https://doi.org/10.1002/asl.304>

14 Ohba, M., & Ueda, H. (2009). Role of nonlinear atmospheric response to SST on the asymmetric  
15 transition process of ENSO. *Journal of Climate*, 22(1), 177–192. <https://doi.org/10.1175/2008JCLI2334.1>

16 Ohba, M., Shiogama, H., Yokohata, T., & Watanabe, M. (2013). Impact of strong tropical volcanic  
17 eruptions on ENSO simulated in a coupled GCM. *Journal of Climate*, 26(14), 5169–5182.  
18 <https://doi.org/10.1175/JCLI-D-12-00471.1>

19 Okumura, Y. M., & Deser, C. (2010). Asymmetry in the duration of El Niño and La Niña. *Journal*  
20 *of Climate*, 23(21), 5826–5843. <https://doi.org/10.1175/2010JCLI3592.1>

21 Oman, L., Robock, A., Stenchikov, G. L., Schmidt, G. A., & Ruedy, R. (2005). Climatic response  
22 to high-latitude volcanic eruptions. *Journal of Geophysical Research: Atmospheres*, 110(D13).  
23 <https://doi.org/10.1029/2004JD005487>

24 Oman, L., Robock, A., Stenchikov, G. L., & Thordarson, T. (2006). High-latitude eruptions cast  
25 shadow over the African monsoon and the flow of the Nile. *Geophysical Research Letters*, 33(18).  
26 <https://doi.org/10.1029/2006GL027665>

27 Osipov, S., Dogar, M. M., & Stenchikov, G. (2016, April). Study of Regional Volcanic Impact on  
28 the Middle East and North Africa using high-resolution global and regional models. In *EGU*  
29 *general assembly conference abstracts* (pp. EPSC2016-8617).

30 Orihuela-Pinto, B., England, M. H., & Taschetto, A. S. (2022). Interbasin and interhemispheric  
31 impacts of a collapsed Atlantic Overturning Circulation. *Nature Climate Change*, 1-8.

32 Otto-Bliesner, B. L., Brady, E. C., Fasullo, J., Jahn, A., Landrum, L., Stevenson, S., ... & Strand, G. (2016).  
33 Climate variability and change since 850 CE: An ensemble approach with the Community Earth System  
34 Model. *Bulletin of the American Meteorological Society*, 97(5), 735-754.

35 Otterå, O. H., Bentsen, M., Drange, H., & Suo, L. (2010). External forcing as a metronome for  
36 Atlantic multidecadal variability. *Nature Geoscience*, 3(10), 688-694.

37 Pausata, F. S. R., Chafik, L., Caballero, R., & Battisti, D. S. (2015). Impacts of high-latitude  
38 volcanic eruptions on ENSO and AMOC. *Proceedings of the National Academy of Sciences*,  
39 112(45), 13784–13788. <https://doi.org/10.1073/pnas.1509153112>

40 Pausata, F. S. R., Karamperidou, C., Caballero, R., & Battisti, D. S. (2016). ENSO response to  
41 high-latitude volcanic eruptions in the Northern Hemisphere: The role of the initial conditions.  
42 *Geophysical Research Letters*, 43(16), 8694–8702. <https://doi.org/10.1002/2016GL069575>

43 Pausata, F. S., Zanchettin, D., Karamperidou, C., Caballero, R., & Battisti, D. S. (2020). ITCZ shift  
44 and extratropical teleconnections drive ENSO response to volcanic eruptions. *Science advances*,  
45 6(23), eaaz5006.

46 Perlwitz, J., and H.-F. Graf, 1995: The statistical connection between tropospheric and stratospheric  
47 circulation of the northern hemisphere in winter. *J. Climate*, 8, 2281–2295,  
48 [https://doi.org/10.1175/1520-0442\(1995\)008<2281:tscbta>2.0.co;2](https://doi.org/10.1175/1520-0442(1995)008<2281:tscbta>2.0.co;2)

1 Pinto, J. P., Turco, R. P., & Toon, O. B. (2018). Self-limiting physical and chemical effects in  
2 volcanic eruption clouds. *Journal of Geophysical Research: Atmospheres*, 94(D8), 11165–11174.  
3 <https://doi.org/10.1029/JD094iD08p11165>

4 Polo, I., Martin-Rey, M., Rodriguez-Fonseca, B., Kucharski, F., & Mechoso, C. R. (2014).  
5 Processes in the Pacific La Niña onset triggered by the Atlantic Niño. *Climate Dynamics*, 44(1–2),  
6 115–131. <https://doi.org/10.1007/s00382-014-2354-7>

7 Power, S., Delage, F., Chung, C., Kociuba,  
8 G., & Keay, K. (2013). Robust twenty-first-century projections of El Niño and related precipitation  
9 variability. *Nature*, 502(7472), 541–545. <https://doi.org/10.1038/nature12580>

10 Polvani, L. M., & Camargo, S. J. (2020). Scant evidence for a volcanically forced winter warming  
11 over Eurasia following the Krakatau eruption of August 1883. *Atmospheric Chemistry and Physics*,  
12 20(22), 13687–13700.

13 Polvani, L. M., Banerjee, A., & Schmidt, A. (2019). Northern Hemisphere continental winter  
14 warming following the 1991 Mt. Pinatubo eruption: reconciling models and observations.  
15 *Atmospheric Chemistry and Physics*, 19(9), 6351–6366.

16 Predybaylo, E., Stenchikov, G. L., Wittenberg, A. T., & Zeng, F. (2017). Impacts of a Pinatubo-size  
17 volcanic eruption on ENSO. *Journal of Geophysical Research: Atmospheres*, 122(2), 925–947.  
18 <https://doi.org/10.1002/2016JD025796>

19 Raible, C. C., Brönnimann, S., Auchmann, R., Brohan, P., Frölicher, T. L., Graf, H. F., ... &  
20 Wegmann, M. (2016). Tambora 1815 as a test case for high impact volcanic eruptions: Earth  
21 system effects. *Wiley Interdisciplinary Reviews: Climate Change*, 7(4), 569–589.

22 Rampino, M. R., & Self, S. (1984). Sulphur-rich volcanic eruptions and stratospheric aerosols.  
23 *Nature*. <https://doi.org/10.1038/310677a0>

24 Rayner, N. A., Parker, D. E., Horton, E. B., Folland, C. K., Alexander, L. V., Rowell, D. P., et al.  
25 (2003). Global analyses of sea surface temperature, sea ice, and night marine air temperature since  
26 the late nineteenth century. *J. Geophys. Res. Vol.*, 108(D14), 4407. [10.1029/2002JD002670](https://doi.org/10.1029/2002JD002670)

27 Ren, H. L., Scaife, A. A., Dunstone, N., Tian, B., Liu, Y., Ineson, S., ... & MacLachlan, C. (2019).  
28 Seasonal predictability of winter ENSO types in operational dynamical model predictions. *Climate  
29 Dynamics*, 52(7), 3869–3890.

30 Rohde, R., Muller, R. A., Jacobsen, R., Muller, E., Perlmutter, S., et al. (2013). A new estimate of  
31 the average Earth surface land temperature spanning 1753 to 2011. *Geoinfor Geostat: An Overview*,  
32 1, 1.

33 Ruprich-Robert, Y., Msadek, R., Castruccio, F., Yeager, S., Delworth, T., & Danabasoglu, G.  
34 (2017). Assessing the climate impacts of the observed atlantic multidecadal variability using the  
35 GFDL CM2.1 and NCAR CESM1 global coupled models. *Journal of Climate*, 30(8), 2785–2810.  
36 <https://doi.org/10.1175/JCLI-D-16-0127.1>

37 Russell, A. M., & Gnanadesikan, A. (2014). Understanding multidecadal variability in ENSO  
38 amplitude. *Journal of Climate*, 27(11), 4037–4051. <https://doi.org/10.1175/JCLI-D-13-00147.1>

39 Santer, B. D., Bonfils, C., Painter, J. F., Zelinka, M. D., Mears, C., Solomon, S., et al. (2014).  
40 Volcanic contribution to decadal changes in tropospheric temperature. *Nature Geoscience*.  
41 <https://doi.org/10.1038/ngeo2098>

42 Sato, M., Hansen, J. E., McCormick, M. P., & Pollack, J. B. (1993). Stratospheric aerosol optical  
43 depths, 1850–1990. *J. Geophys. Res.*, 98(D12), 22,987–22,994.

44 Schneider, D. P., Ammann, C. M., Otto-Bliesner, B. L., & Kaufman, D. S. (2009). Climate response  
45 to large, high-latitude and low-latitude volcanic eruptions in the Community Climate System  
46 Model. *Journal of Geophysical Research: Atmospheres*, 114(D15).

47 Schneider, T., Bischoff, T., & Haug, G. H. (2014). Migrations and dynamics of the intertropical  
48 convergence zone. *Nature*, 513, 45. Retrieved from <http://dx.doi.org/10.1038/nature13636>

49 Sear, C. B., Kelly, P. M., Jones, P. D., & Goodess, C. M. (1987). Global surface temperature  
50 responses to major volcanic eruptions. *Nature*. <https://doi.org/10.1038/330365a0>

1 Self, S., Rampino, M. R., Zhao, J., & Katz, M. G. (1997). Volcanic aerosol perturbations and strong  
2 El Niño events: No general correlation. *Geophysical Research Letters*, 24(10), 1247–1250.  
3 <https://doi.org/10.1029/97GL01127>

4 Shindell, D. T., Schmidt, G. A., Mann, M. E., & Faluvegi, G. (2004). Dynamic winter climate  
5 response to large tropical volcanic eruptions since 1600. *Journal of Geophysical Research*.  
6 <https://doi.org/10.1029/2003JD004151>

7 Sigl, M., Winstrup, M., McConnell, J. R., Welten, K. C., Plunkett, G., Ludlow, F., et al. (2015).  
8 Timing and climate forcing of volcanic eruptions for the past 2,500 years. *Nature*, 523, 543.

9 Singh et al. (2020) Fingerprint of volcanic forcing on the ENSO-Indian monsoon coupling *Sci.*  
10 *Adv.*; 6 : eaba8164

11 Soden, B. J., Wetherald, R. T., Stenchikov, G. L., & Robock, A. (2002). Global cooling after the  
12 eruption of Mount Pinatubo: A test of climate feedback by water vapor. *Science*, 296(5568), 727  
13 LP-730. Retrieved from [http://science.sciencemag.org/  
14 content/296/5568/727.abstract](http://science.sciencemag.org/content/296/5568/727.abstract)

15 Stahle, D. S., D'Arrigo, R. D., Krusic, P. J., Cleaveland, M. K., Cook, E. R., Allan, R. J., et al.  
16 (1998). Experimental dendroclimatic reconstruction of the Southern Oscillation. *Bulletin of the*  
17 *American Meteorological Society*, 79(10), 2137–2152. [https://doi.org/10.1175/1520-  
18 0477\(1998\)079<2137:EDROTS>2.0.CO;2](https://doi.org/10.1175/1520-0477(1998)079<2137:EDROTS>2.0.CO;2)

19 Stenchikov, G. L., Kirchner, I., Robock, A., Graf, H. F., Antuña, J. C., Grainger, R. G., et al.  
20 (1998). Radiative from the 1991 Mount Pinatubo volcanic eruption. *Journal of Geophysical*  
21 *Research*, 103(D12), 13,837-13,857.

22 Stenchikov, G., A. Robock, V. Ramaswamy, M. D. Schwarzkopf, K. Hamilton, and S.  
23 Ramachandran, 2002: Arctic Oscillation response to the 1991 Mount Pinatubo eruption: Effects of  
24 volcanic aerosols and ozone depletion. *J. Geophys. Res.*, 107, 4803,  
25 <https://doi.org/10.1029/2002jd002090>.

26 Stenchikov, G., Hamilton, K., Robock, A., Ramaswamy, V., and Schwarzkopf, M. D. (2004).  
27 Arctic oscillation response to the 1991 Pinatubo eruption in the SKYHI general circulation model  
28 with a realistic quasi - biennial oscillation, *J. Geophys. Res.*, 109, D03112,  
29 [doi:10.1029/2003JD003699](https://doi.org/10.1029/2003JD003699).

30 Stenchikov, G., Hamilton, K., Stouffer, R. J., Robock, A., Ramaswamy, V., Santer, B., & Graf, H.-  
31 F. (2006). Arctic Oscillation response to volcanic eruptions in the IPCC AR4 climate models. *J.*  
32 *Geophys. Res.*, 111, D07107. [doi:10.1029/2005JD006286](https://doi.org/10.1029/2005JD006286)

33 Stenchikov, G. L., Delworth, T. L., Ramaswamy, V., Stouffer, R. J., Wittenberg, A., & Zeng, F.  
34 (2009). Volcanic signals in oceans. *Journal of Geophysical Research Atmospheres*, 114(16), 1–13.  
35 <https://doi.org/10.1029/2008JD011673>

36 Stevenson, S., Otto-Bliesner, B., Fasullo, J., & Brady, E. (2016). “El Niño Like” hydroclimate  
37 responses to last millennium volcanic eruptions. *Journal of Climate*, 29(8), 2907–2921.  
38 <https://doi.org/10.1175/JCLI-D-15-0239.1>

39 Stevenson, S., Fasullo, J. T., Otto-Bliesner, B. L., Tomas, R. A., & Gao, C. (2017). Role of eruption  
40 season in reconciling model and proxy responses to tropical volcanism. *Proceedings of the National*  
41 *Academy of Sciences*, 114(8), 1822–1826. <https://doi.org/10.1073/pnas.1612505114>

42 Stoffel, M., Khodri, M., Corona, C., Guillet, S., Poulain, V., Bekki, S., et al. (2015). Estimates of  
43 volcanic-induced cooling in the Northern Hemisphere over the past 1,500 years. *Nature Geoscience*,  
44 8, 784. Retrieved from [https://doi.org/10.1038/  
45 ngeo2526](https://doi.org/10.1038/ngeo2526)

46 Sutton, R. T., Dong, B., & Gregory, J. M. (2007). Land/sea warming ratio in response to climate  
47 change: IPCC AR4 model results and comparison with observations. *Geophysical Research Letters*,  
48 34(2). <https://doi.org/10.1029/2006GL028164>

49 Swingedouw, D., Ortega, P., Mignot, J., Guilyardi, E., MassonDelmotte, V., Butler, P. G., et al.  
50 (2015). Bidecadal North Atlantic ocean circulation variability controlled by timing of volcanic  
eruptions. *Nature Communications*, 6, 6545. Retrieved from  
<https://doi.org/10.1038/ncomms7545>

1 Swingedouw, D., Mignot, J., Ortega, P., Khodri, M., Menegoz, M., Cassou, C., & Hanquiez, V.  
2 (2017). Impact of explosive volcanic eruptions on the main climate variability modes. *Global and*  
3 *Planetary Change*, 150, 24–45. [https://doi.org/](https://doi.org/10.1016/j.gloplacha.2017.01.006) <https://doi.org/10.1016/j.gloplacha.2017.01.006>  
4 Taschetto, A. S., Ummenhofer, C. C., Stuecker, M. F., Dommenges, D., Ashok, K., Rodrigues, R.  
5 R., & Yeh, S. W. (2020). ENSO atmospheric teleconnections. *El Niño southern oscillation in a*  
6 *changing climate*, 309-335.  
7 Tejedor, E., Steiger, N. J., Smerdon, J. E., Serrano-Notivol, R., & Vuille, M. (2021). Global  
8 hydroclimatic response to tropical volcanic eruptions over the last millennium. *Proceedings of the*  
9 *National Academy of Sciences*, 118(12).  
10 Stenchikov, G., A. Robock, V. Ramaswamy, M. D. Schwarzkopf, K. Hamilton, and S.  
11 Ramachandran, 2002: Arctic Oscillation response to the 1991 Mount Pinatubo eruption: Effects of  
12 volcanic aerosols and ozone depletion. *J. Geophys. Res.*, 107, 4803,  
13 <https://doi.org/10.1029/2002jd002090>.  
14 Ropelewski, C. F., & Halpert, M. S. (1986). North American precipitation and temperature patterns  
15 associated with the El Niño/Southern Oscillation (ENSO). *Monthly Weather Review*, 114(12),  
16 2352-2362.  
17 Thompson, D. W. J., & Solomon, S. (2009) Understanding recent stratospheric climate change. *J.*  
18 *Climate*, 22, 1934–1943. doi:10.1175/2008JCLI2482.1  
19 Thompson, D. W. J., Wallace, J. M., Jones, P. D., & Kennedy, J. J. (2009). Identifying signatures of  
20 natural climate variability in time series of global-mean surface temperature: Methodology and  
21 insights. *Journal of Climate*. <https://doi.org/10.1175/2009JCLI3089.1>  
22 Tierney, J. E., Abram, N. J., Anchukaitis, K. J., Evans, M. N., Giry, C., Kilbourne, K. H., et al.  
23 (2015). Tropical sea surface temperatures for the past four centuries reconstructed from coral  
24 archives. *Paleoceanography*, 30(3), 226–252. <https://doi.org/10.1002/2014PA002717>  
25 Timmermann, A., An, S. I., Krebs, U., & Goosse, H. (2005). ENSO suppression due to weakening  
26 of the North Atlantic thermohaline circulation. *Journal of Climate*, 18(16), 3122– 3139.  
27 <https://doi.org/10.1175/JCLI3495.1>  
28 Timmermann, A., Okumura, Y., An, S. I., Clement, A., Dong, B., Guilyardi, E., et al. (2007). The  
29 influence of a weakening of the Atlantic meridional overturning circulation on ENSO. *Journal of*  
30 *Climate*, 20(19), 4899–4919. <https://doi.org/10.1175/JCLI4283.1>  
31 Timmreck, C. (2012). Modeling the climatic effects of large explosive volcanic eruptions. *Wiley*  
32 *Interdisciplinary Reviews: Climate Change*, 3(6), 545–564. <https://doi.org/10.1002/wcc.192>  
33 Timmreck, C., Lorenz, S. J., Crowley, T. J., Kinne, S., Raddatz, T. J., Thomas, M. A., & Jungclaus,  
34 J. H. (2009). Limited temperature response to the very large AD 1258 volcanic eruption.  
35 *Geophysical Research Letters*, 36(21).  
36 Timmreck, C., Mann, G. W., Aquila, V., Hommel, R., Lee, L. A., Schmidt, A., et al. (2018). The  
37 Interactive Stratospheric Aerosol Model Intercomparison Project (ISA-MIP): Motivation and  
38 experimental design. *Geoscientific Model Development*, 11(7), 2581–2608. [https://doi.org/10.5194/](https://doi.org/10.5194/gmd-11-2581-2018)  
39 [gmd-11-2581-2018](https://doi.org/10.5194/gmd-11-2581-2018)  
40 Timmreck, C., H. Pohlmann, S. Illing, and C. Kadow (2016), The impact of stratospheric volcanic  
41 aerosol on decadal-scale climate predictions, *Geophys. Res. Lett.*, 43, doi:10.1002/2015GL067431.  
42 Toohey, M., Krüger, K., Niemeier, U., & Timmreck, C. (2011). The influence of eruption season on  
43 the global aerosol evolution and radiative impact of tropical volcanic eruptions. *Atmospheric*  
44 *Chemistry and Physics*, 11(23), 12351–12367. <https://doi.org/10.5194/acp-11-12351-2011>  
45 Toohey, M., Stevens, B., Schmidt, H., & Timmreck, C. (2016). Easy Volcanic Aerosol (EVA v1.0):  
46 An idealized forcing generator for climate simulations. *Geoscientific Model Development*, 9(11),  
47 4049–4070. <https://doi.org/10.5194/gmd-9-4049-2016>.  
48 Trenberth, K. E., and J. M. Caron (2000), The Southern Oscillation revisited: Sea level pressures,  
49 surface temperatures, and precipitation, *J. Clim.*, 13(24), 4358–4365.  
50 Trenberth, K. E., and A. Dai (2007), Effects of Mount Pinatubo volcanic eruption on the  
51 hydrological cycle as an analog of geoengineering, *Geophys. Res. Lett.*, 34, L15702,  
52 doi:10.1029/2007GL030524.

1 Trepte, C. R., R. E. Veiga, and M. P. McCormick (1993). The poleward dispersal of Mount  
2 Pinatubo volcanic aerosol. *J. Geophys. Res.*, 98(D10), 18, 563–18, 573, doi:10.1029/93JD01362  
3 Vijayeta, A., & Dommenges, D. (2018). An evaluation of ENSO dynamics in CMIP simulations in  
4 the framework of the recharge oscillator model. *Climate Dynamics*, 51(5), 1753– 1771.  
5 <https://doi.org/10.1007/s00382-017-3981-6>  
6 Ward, B., Pausata, F. S., & Maher, N. (2020). The sensitivity of the ENSO to volcanic aerosol  
7 spatial distribution in the MPI large ensemble. *Earth System Dynamics Discussions*, 1-28.  
8 Wilson, R., Cook, E., D'Arrigo, R., Riedwyl, N., Evans, M. N., Tudhope, A., & Allan, R. (2010).  
9 Reconstructing ENSO: The influence of method, proxy data, climate forcing and teleconnections.  
10 *Journal of Quaternary Science*, 25(1), 62–78. <https://doi.org/10.1002/jqs.1297>  
11 Wu et al (2021). Two-year Dynamical Predictions of ENSO Event Duration during 1954–2015. *J.*  
12 *Clim.*,  
13 Wang, T., D. Guo, Y. Q. Gao, H. Wang, F. Zheng, Y. Zhu, J. Miao, and Y. Hu, 2018: Modulation  
14 of ENSO evolution by strong tropical volcanic eruptions. *Climate Dyn.*, 51, 2433–2453,  
15 <https://doi.org/10.1007/s00382-017-4021-2>.  
16 Wunderlich, F. and Mitchell, D. M.: Revisiting the observed surface climate response to large  
17 volcanic eruptions, *Atmospheric Chemistry and Physics*, 17, 485–499.  
18 Xie, S. P., Deser, C., Vecchi, G. A., Ma, J., Teng, H., & Wittenberg, A. T. (2010). Global warming  
19 pattern formation: Sea surface temperature and rainfall. *Journal of Climate*, 23(4), 966–986.  
20 <https://doi.org/10.1175/2009JCLI3329.1>  
21 Xing, C., Liu, F., Wang, B., Chen, D., Liu, J., & Liu, B. (2020). Boreal Winter Surface Air  
22 Temperature Responses to Large Tropical Volcanic Eruptions in CMIP5 Models. *Journal of*  
23 *Climate*, 33(6), 2407-2426.  
24 Yang, L., Gao, Y., Gao, C., & Liu, F. (2022). Climate Responses to Tambora-Size Volcanic  
25 Eruption and the Impact of Warming Climate. *Geophysical Research Letters*, 49(10),  
26 e2021GL097477.  
27 Yu, R., and T. Zhou (2004), Impacts of winter-NAO on March cooling trends over subtropical  
28 Eurasia continent in the recent half century, *Geophysical Research Letters*, 31(12),  
29 doi:10.1029/2004GL019814.  
30 Zambri, B., LeGrande, A. N., Robock, A., & Slawinska, J. (2017). Northern Hemisphere winter  
31 warming and summer monsoon reduction after volcanic eruptions over the last millennium. *Journal*  
32 *of Geophysical Research: Atmospheres*, 122(15), 7971-7989.  
33 Zanchettin, D., Timmreck, C., Graf, H.-F., Rubino, A., Lorenz, S., Lohmann, K., et al. (2012). Bi-  
34 decadal variability excited in the coupled ocean–atmosphere system by strong tropical volcanic  
35 eruptions. *Climate Dynamics*, 39(1), 419–444. <https://doi.org/10.1007/s00382-011-1167-1>  
36 Zanchettin, D., Khodri, M., Timmreck, C., Toohey, M., Schmidt, A., Gerber, E. P., et al. (2016).  
37 The Model Intercomparison Project on the climatic response to volcanic forcing (VolMIP):  
38 Experimental design and forcing input data for CMIP6. *Geoscientific Model Development*, 9(8),  
39 2701–2719. <https://doi.org/10.5194/gmd-9-2701-2016>  
40 Zebiak, S. E., & Cane, M. A. (1987). A model El Niño–Southern Oscillation. *Monthly Weather*  
41 *Review*. [https://doi.org/10.1175/1520-0493\(1987\)115<2262:AMENO>2.0.CO;2](https://doi.org/10.1175/1520-0493(1987)115<2262:AMENO>2.0.CO;2)  
42 Zeng, N. (2003). Drought in the Sahel. *Science*, 302(5647), 999-1000.  
43 Zhang, R., & Delworth, T. L. (2005). Simulated tropical response to a substantial weakening of the  
44 Atlantic thermohaline circulation. *Journal of Climate*, 18(12), 1853–1860.  
45 <https://doi.org/10.1175/JCLI3460.1>  
46 Zhang, D., R. Blender, and K. Fraedrich (2013), Volcanoes and ENSO in millennium simulations:  
47 Global impacts and regional reconstructions in East Asia, *Theor. Appl. Climatol.*, 111(3–4), 437–  
48 454.  
49 Zhang, W., F.-F. Jin, J.-X. Zhao, L. Qi, and H.-L. Ren (2013), The possible influence of a  
50 nonconventional El Niño on the severe autumn drought of 2009 in Southwest China, *J. Clim.*,  
51 26(21), 8392–8405.

1 Zhu, F., Emile-Geay, J., Anchukaitis, K., Hakim, G., Wittenberg, A., Morales, M., & King, J.  
2 (2021). Volcanoes and ENSO: a re-appraisal with the Last Millennium Reanalysis.  
3 Zhu, F., Emile-Geay, J., Anchukaitis, K. J., Hakim, G. J., Wittenberg, A. T., Morales, M. S., ... &  
4 King, J. (2022). A re-appraisal of the ENSO response to volcanism with paleoclimate data  
5 assimilation. *Nature Communications*, 13(1), 1-9.  
6 Zhu, Y., Toon, O. B., Jensen, E. J., Bardeen, C. G., Mills, M. J., Tolbert, M. A., ... & Woods, S.  
7 (2020). Persisting volcanic ash particles impact stratospheric SO<sub>2</sub> lifetime and aerosol optical  
8 properties. *Nature communications*, 11(1), 1-11.  
9 Zhuo, Z., Kirchner, I., Pfahl, S., & Cubasch, U. (2021). Climate impact of volcanic eruptions: the  
10 sensitivity to eruption season and latitude in MPI-ESM ensemble experiments. *Atmospheric*  
11 *Chemistry and Physics*, 21(17), 13425-13442.  
12 Zuo, M., Man, W., Zhou, T., & Guo, Z. (2018). Different impacts of northern, tropical, and  
13 southern volcanic eruptions on the tropical Pacific SST in the last millennium. *Journal of Climate*,  
14 31(17), 6729–6744. <https://doi.org/10.1175/JCLI-D-17-0571.1>  
15 Zuo, M., Zhou, T., & Man, W. (2021). Dependence of global monsoon response to volcanic  
16 eruptions on the background oceanic states. *Journal of Climate*, [https://doi.org/10.1175/JCLI-D-20-](https://doi.org/10.1175/JCLI-D-20-0891.1)  
17 0891.1  
18  
19  
20

21 **Table 1:** Details of the ENSO reconstructions, and their correlation with the observed ENSO variability  
22 as denoted by the Southern-Oscillation Index (SOI) over the period 1900–1977 (Source: McGregor et al.  
23 2020).  
24

Proxy Number	Start Year	End Year	Reference	Source Proxy Location	Source Proxy Type	Correlation with SOI
1	1706	1997	Stahle et al. (1998)	Pacific Basin	Tree ring	0.76
2	1408	1978	Cook (2000)	North America	Tree ring	0.73
3	1650	1990	Mann et al. (2000)	Near global tropics	Mixed	0.78
4	1590	1990	Evans et al. (2002)	Indo-Pacific Basin	Coral	0.67
5	1800	1990	Evans et al. (2001)	America	Tree ring	0.67
6	1300	1978	Cook et al. (2008)	North America	Tree ring	0.75
7	1727	1982	Braganza et al. (2009)	Pacific Basin	Mixed	0.73
8	1525	1982	Braganza et al. (2009)	Pacific Basin	Mixed	0.65
9	1650	1977	McGregor et al. (2010)	Pacific Basin	Mixed	0.83
10	1607	1998	Wilson et al. (2010)	Tropical Pacific	Mixed	0.58
11	1540	1998	Wilson et al. (2010)	Pacific Basin	Mixed	0.48
12	900	2002	Li et al. (2011)	North America	Tree ring	0.6
13	1150	1998	Emile-Geay et al. (2013a, 2013b)	Near global tropics	Mixed	0.8
14	1150	1998	Emile-Geay et al. (2013a, 2013b)	Near global tropics	Mixed	0.83
15	1150	1998	Emile-Geay et al. (2013a, 2013b)	Near global tropics	Mixed	0.82
16	1301	2005	Li et al. (2013)	Pacific Basin	Tree ring	0.67
17	1607	1997	Tierney et al. (2015)	Tropical Pacific	Coral	0.74

25

26 **Figure Legends:**

27 **Figure 1:** Observed SST response to the five main volcanic eruptions during 1870–2010 (i.e., Krakatau  
28 (1883), Santa Maria (1902), Mt Agung (1962), El Chichon (1982), and Pinatubo (1991)). SST anomalies  
29 (SSTA, °C) are computed using the preceding 5-year climatology, and the resulting anomalies are plotted  
30 relative to the tropical average (20°N–20°S). (a) Evolution of the composited Niño-3.4 (5°S–5°N,  
31 170°W–120°W) SSTA plotted over the 2-year period including the five largest volcanic eruptions during  
32 1870–2010 in HadISST observations (black line). The red dots denote when the five events have  
33 anomalies of the same sign. An arrow indicates the dates and magnitude of the selected eruptions, based

1 on AOD by Gao et al. (2008). (b) Same as (a) but shown as a longitude-time section. The black rectangle  
2 denotes the Niño-3.4 region during October–November–December. Stippling highlights times and  
3 locations where the five eruptions display anomalies of the same sign and the contour corresponds to the  
4 90% significance level of this anomaly following a two-tailed Student’s *t*-test. Note that the composites  
5 maintained a common seasonality (i.e., the calendar months of each eruption were aligned despite the  
6 differing eruption months) due to the seasonally synchronized nature of ENSO dynamics (Source: Khodri et  
7 al. 2017).

8 **Figure 2:** Observed boreal-winter SAT anomaly after the five strong volcanic events (Krakatau, Santa  
9 María, Agung, El Chichón, and Pinatubo). Composite SAT anomaly (shading; K) with respect to the five  
10 years preceding each eruption during the first boreal winter after the five selected eruptions in (a) 20CRv2c,  
11 (b) GISTEMP. Stippling indicates temperature anomaly significant at the 95% confidence level.

12 **Figure 3:** Observed and simulated El Niño relationship with volcanism. Five month running mean of Niño  
13 3.4 index (K; dotted line: HadSST1; solid line: HadSST2; dot-dashed line: ERSSTv5) and 850 hPa WCEP  
14 (140° E–180°, 5° S–5° N) zonal wind (U, ms<sup>-1</sup>) anomalies in observations and reanalysis and in SEA  
15 composite of 41 ensemble members of CESM-LE (dashed line) for Agung (1963), El Chichón (1982), and  
16 Pinatubo (1991) eruptions. Solid part of the curve denotes simulated anomaly significant above the 95%  
17 confidence level. Monthly zonal-mean AOD before and after the eruptions for these eruptions are obtained  
18 from Ammann (2003). Year (0) denotes the eruption year, and year (1) is the first year after the eruption  
19 (Source: Chai et al. 2020).

20 **Figure 4:** Superposed Epoch Analysis of the last millennium reanalysis (LMR) Niño 3.4 reconstructions  
21 around the 13 events when the Palmyra coral record is available, a) coral predictors only, b) six best  
22 tree-ring based Niño 3.4 predictors previously identified by Li et al. 2013 (Li13b6), and c)  
23 corals+Li13b6 predictors. Solid curves with dark dots denote the composite mean, and the light dots  
24 denote the Niño 3.4 anomaly at each year for each individual event. The light gray dashed curves denote  
25 the 1%, 5%, 10%, 90%, 95%, and 99% quantiles of the composite means from 1000 bootstrap drawn  
26 from non-volcanic years (Zhu et al. 2022).

27 **Figure 5:** Composited ensemble-mean seasonal average surface temperature anomalies (relative to  
28 tropical mean: 20°N–20°S) and rainfall anomalies (contours at intervals of 0.2 mm/day; zero contours  
29 are excluded) with surface wind (m/s; vector). The ensemble mean maps are calculated from 32 CMIP5  
30 models that are each composited around five strong volcanic events (i.e., Krakatau, Santa María, Agung,  
31 El Chichón, and Pinatubo) where the eruption begins in year 0. DJF (0/1) is peak of the strong tropical  
32 volcanic forcing composite (Source: McGregor et al. 2020).

33 **Figure 6:** Transition to La Niña from tropical eruption-induced El Niño mode and internal El Niño  
34 mode. Shown are the composite NINO3 index for 25 tropical eruptions during the period 501 to 2000  
35 AD (thick red line) and for the El Niño in the control run (thick blue line), as well as the associated zonal  
36 wind anomalies (dashed lines) averaged over the western Pacific (5°S–5°N, 120°E–150°E). “1” denotes  
37 1 year after each eruption, and “2”, 2 years. The El Niño in the control run is defined when the boreal  
38 winter (December–February average) NINO index is above one standard deviation. Each variable is  
39 normalized by its maximum value in years “1” and “2”. The year is defined as the eruption year when its  
40 annual aerosol is larger than the 2 years before and after it. When the eruption starts late in the year, e.g.,  
41 November or December, it has maximum aerosol density in the following year; in such case, the  
42 following year is considered as the eruption year (Source: Liu et al. 2018).

44 **Figure 7:** CESM version 1.0 (CESM1) model simulated SST anomaly evolutions after different eruptions.  
45 The composites of normalized 3-month-mean SST anomalies (shading), and 850-hPa wind anomalies  
46 (vectors) since the first winter after the NH (a), the tropical (b), and the SH (c) eruptions. “0” denotes the  
47 year of each eruption, and “+1” indicates 1 year after the eruption.

48 **Figure 8:** CESM version 1.0 (CESM1) model simulated oceanic responses to different eruptions. The  
49 normalized composite summer-mean (June–August) surface currents and surface (0–20 m) upwelling  
50 anomalies one year after the NH (a), the tropical (b), and the SH (c) eruptions (Source: Liu et al. 2018).

51 **Figure 9:** Stratospheric responses to tropical volcanism in CMIP6. Composites of (a) zonally averaged  
52 temperature anomalies as a function of latitude and height (shading), and (b) 50-hPa geopotential height  
53 anomalies in the first NH winter following the five tropical eruptions for the multi-model mean of the 21



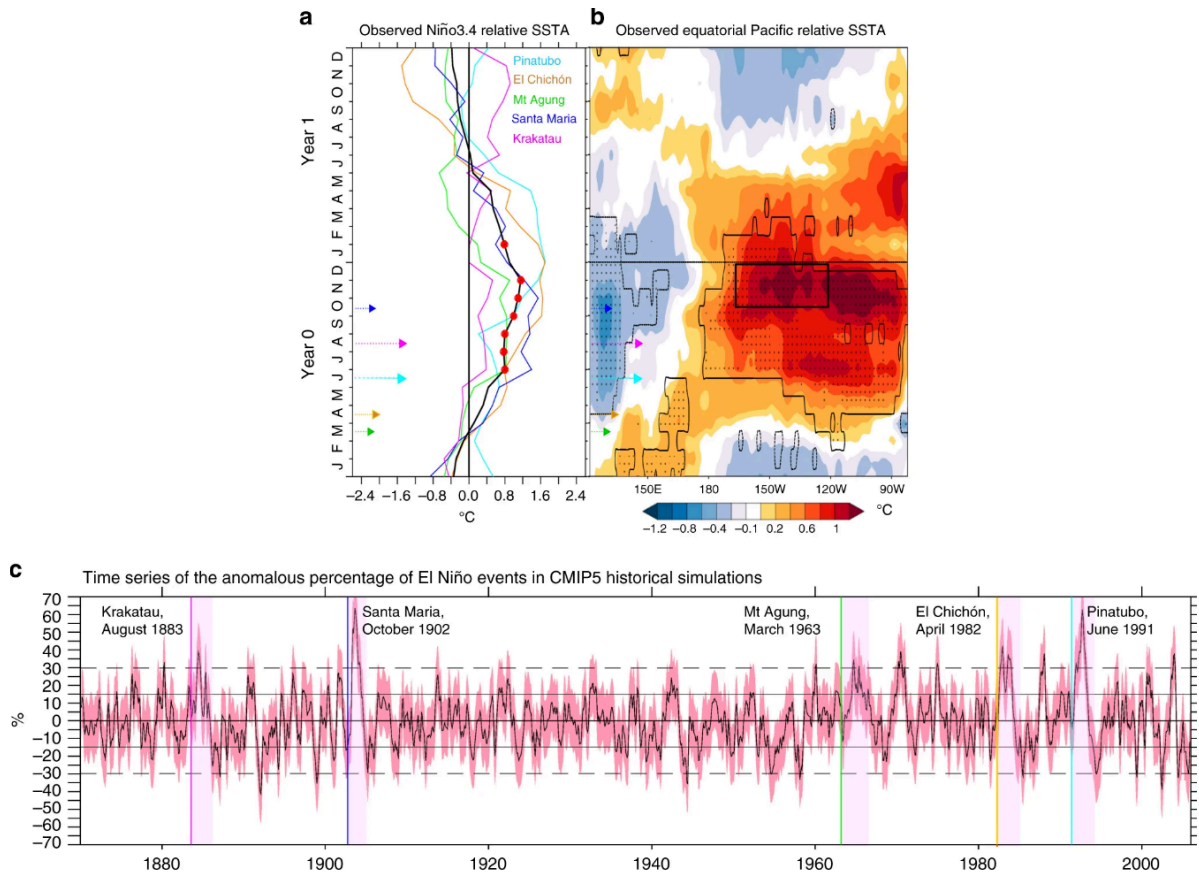
1 CMIP6 models (shading). The ensemble mean of each model is also shown in (b). Stippling denotes  
2 anomalies significant at the 95% confidence level (Source: Liu et al. 2020).

3  
4 **Figure 10:** A schematic diagram suggesting two different experiments using a large number of coupled  
5 GCMs with large ensemble members with volcanic (i.e., panel A) and non-volcanic forcing (i.e., panel B).  
6 The difference of the ensemble average of these multi-model, multi-ensemble volcanic forcing experiments  
7 from non-volcanic experiments is required to delineate the volcanic impact (i.e., direct and non-direct) from  
8 natural climate variability. Large-scale circulation changes that supposedly play role in high-latitude winter  
9 warming are shown in bold red font.

10

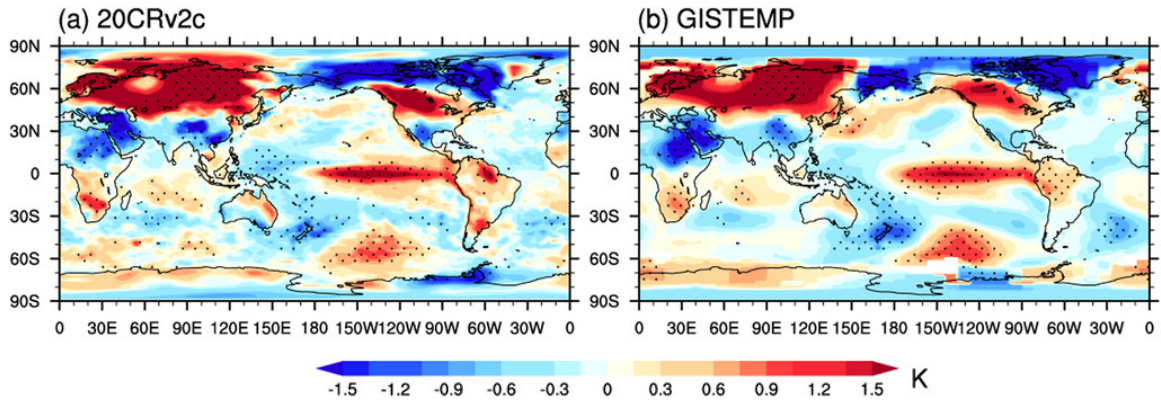
11

1  
2



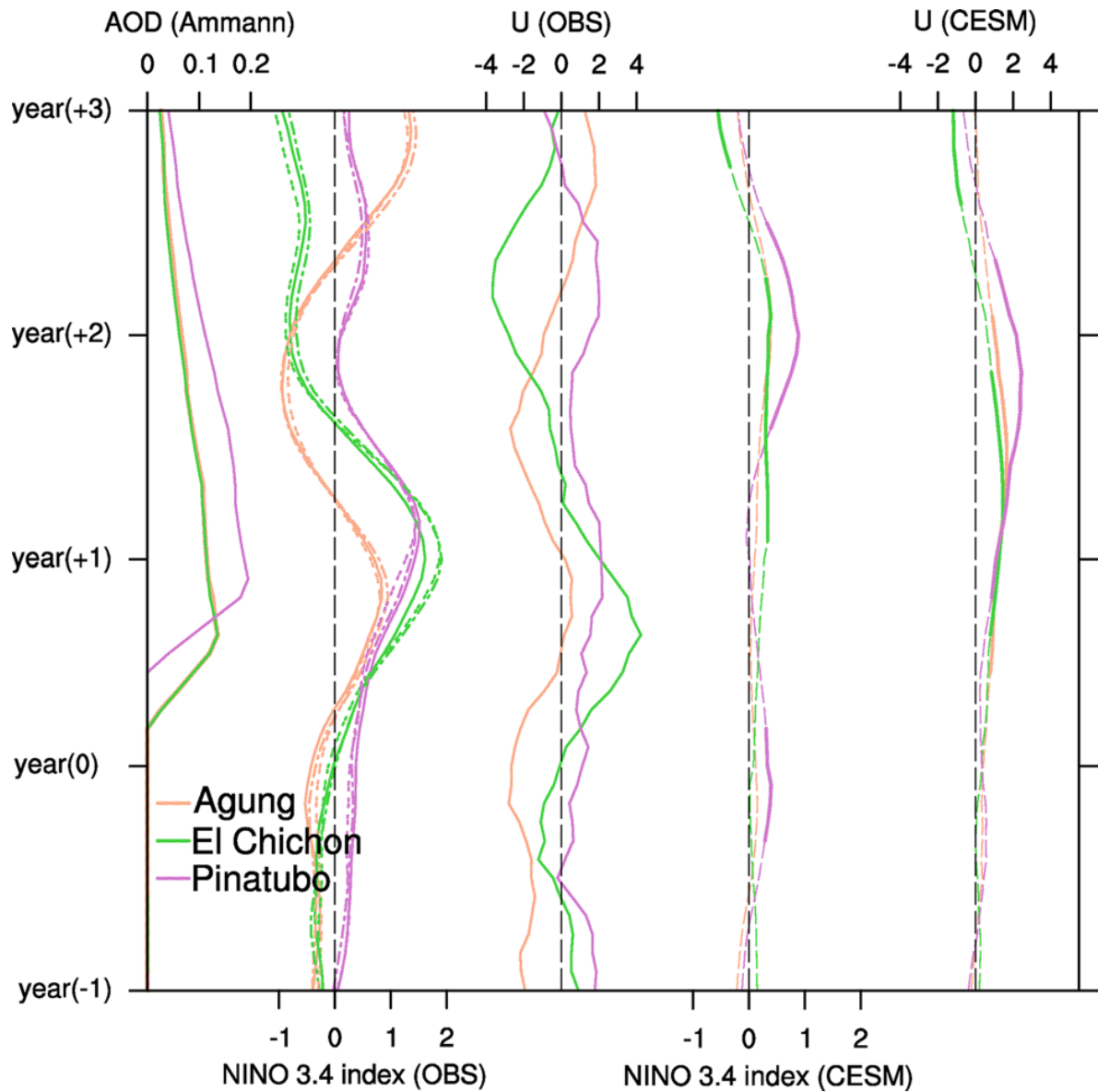
3

4 **Figure 1:** Observed SST response to the five main volcanic eruptions during 1870–2010 (i.e., Krakatau  
5 (1883), Santa Maria (1902), Mt Agung (1962), El Chichon (1982), and Pinatubo (1991)). SST anomalies  
6 (SSTA, °C) are computed using the preceding 5-year climatology, and the resulting anomalies are plotted  
7 relative to the tropical average (20°N–20°S). (a) Evolution of the composited Niño-3.4 (5°S–5°N,  
8 170°W–120°W) SSTA plotted over the 2-year period including the five largest volcanic eruptions during  
9 1870–2010 in HadISST observations (black line). The red dots denote when the five events have  
10 anomalies of the same sign. An arrow indicates the dates and magnitude of the selected eruptions, based  
11 on AOD by Gao et al. (2008). (b) Same as (a) but shown as a longitude-time section. The black rectangle  
12 denotes the Niño-3.4 region during October–November–December. Stippling highlights times and  
13 locations where the five eruptions display anomalies of the same sign and the contour corresponds to the  
14 90% significance level of this anomaly following a two-tailed Student’s *t*-test. (c) Time series of  
15 anomalous percentage of El Niño occurrence for CMIP5 historical simulation members over the entire  
16 historical period (136 years). Note that the composites maintained a common seasonality due to the  
17 seasonally synchronized nature of ENSO events (Reproduced from Khodri et al. (2017) under a creative  
18 commons attribution 4.0 license <https://creativecommons.org/licenses/by/4.0/>).



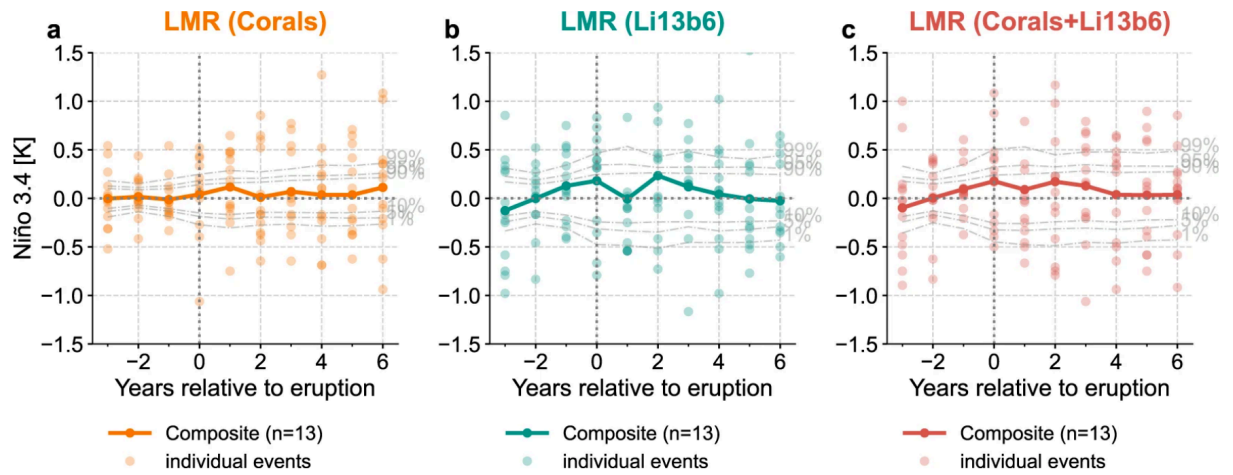
1  
2  
3  
4  
5  
6  
7  
8

**Figure 2:** Observed boreal-winter SAT anomaly (K) after the five strong volcanic events (Krakatau, Santa María, Agung, El Chichón, and Pinatubo). Composite SAT anomaly (shading; K) with respect to the five years preceding each eruption during the first boreal winter after the five selected eruptions in (a) 20CRv2c, (b) GISTEMP. Stippling indicates temperature anomaly significant at the 95% confidence level (Reproduced from Xing et al. (2020). © 2018 American Meteorological Society, used with permission).



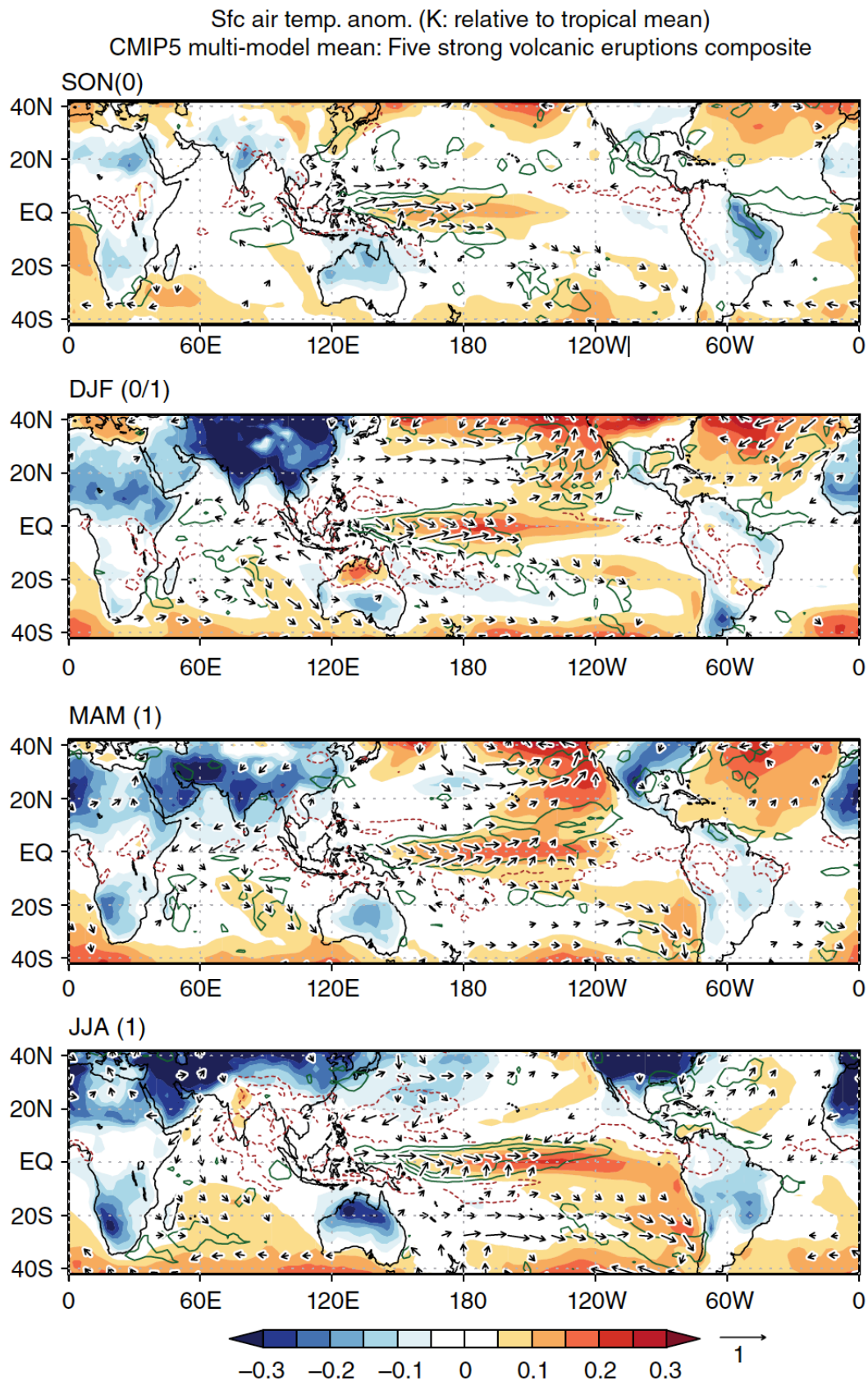
1  
2  
3  
4  
5  
6  
7  
8  
9  
10  
11  
12  
13  
14  
15  
16  
17  
18

**Figure 3:** Observed and simulated El Niño relationship with volcanism. Five month running mean of Niño 3.4 index (K; dotted line: HadSST1; solid line: HadSST2; dot-dashed line: ERSSTv5) and 850 hPa WCEP (140° E–180°, 5° S–5° N) zonal wind (U, ms<sup>-1</sup>) anomalies in observations and reanalysis and in SEA composite of 41 ensemble members of CESM-LE (dashed line) for Agung (1963), El Chichón (1982), and Pinatubo (1991) eruptions. Solid part of the curve denotes simulated anomaly significant above the 95% confidence level. Monthly zonal-mean AOD before and after the eruptions for these eruptions are obtained from Ammann (2003). Year (0) denotes the eruption year, and year (1) is the first year after the eruption (Reproduced from Chai et al. (2020) under a creative commons attribution 4.0 license <https://creativecommons.org/licenses/by/4.0/>).



1  
2  
3  
4  
5  
6  
7  
8  
9

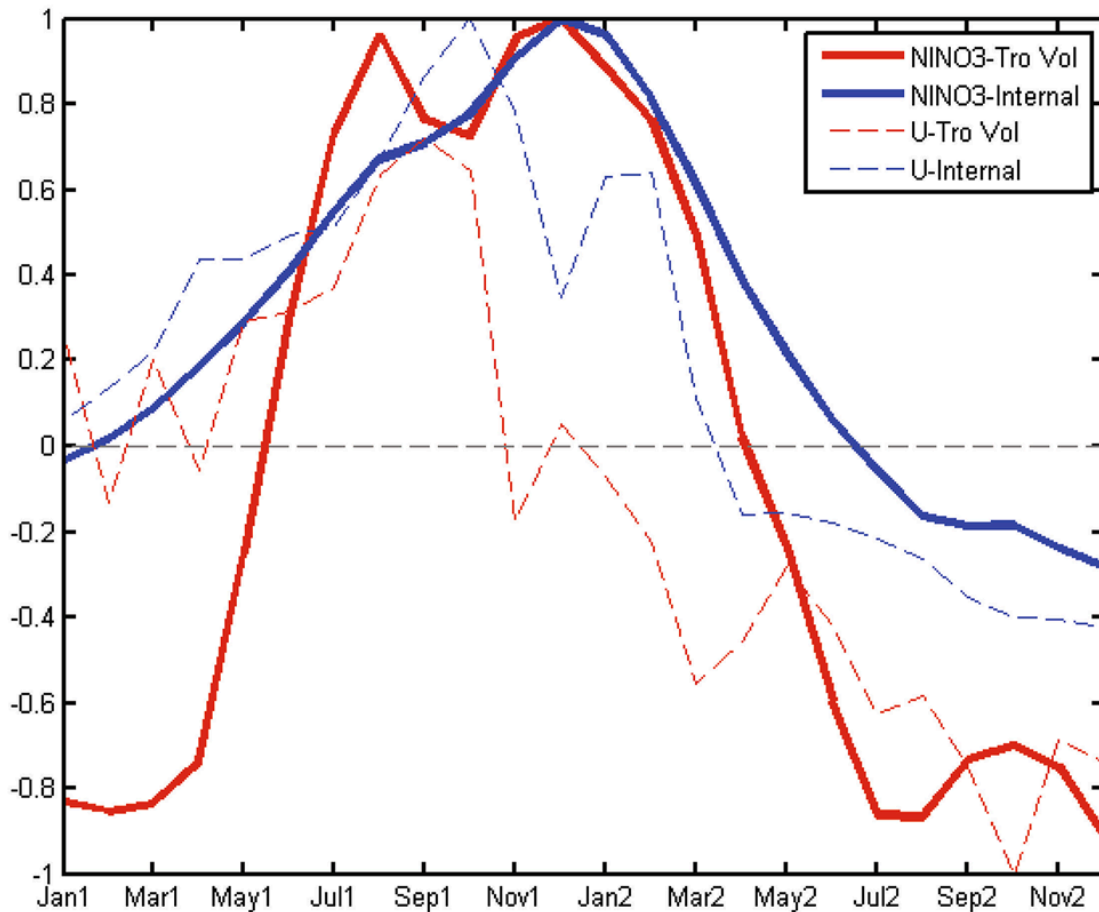
**Figure 4:** Superposed Epoch Analysis of the last millennium reanalysis (LMR) Niño 3.4 reconstructions around the 13 events when the Palmyra coral record is available, a) coral predictors only, b) six best tree-ring based Niño 3.4 predictors previously identified by Li et al. 2013 (Li13b6), and c) corals+Li13b6 predictors. Solid curves with dark dots denote the composite mean, and the light dots denote the Niño 3.4 anomaly at each year for each distinct event. The light gray dashed curves denote the 1%, 5%, 10%, 90%, 95%, and 99% quantiles of the composite means from 1000 bootstrap drawn from non-volcanic years (Reproduced from Zhu et al. (2022) under a creative commons attribution 4.0 license <https://creativecommons.org/licenses/by/4.0/>).



1  
 2  
 3  
 4  
 5

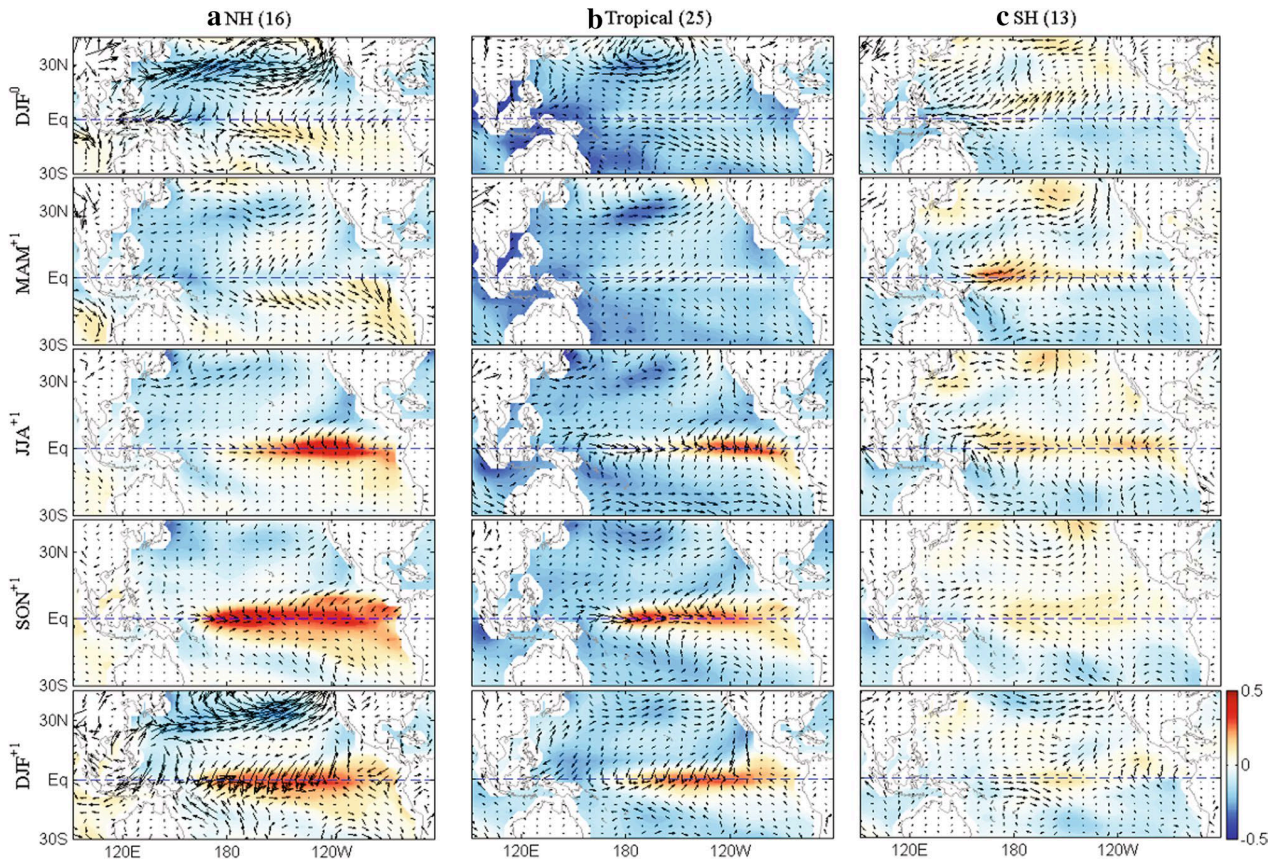
**Figure 5:** Composited ensemble-mean seasonal average surface temperature anomalies (relative to tropical mean: 20°N–20°S, unit: K) and rainfall anomalies (contours at intervals of 0.2 mm/day; zero contours are excluded) with surface wind (m/s; vector). The ensemble mean maps are calculated from 32 CMIP5 models that are each composited around five strong volcanic events (i.e., Krakatau, Santa Maria,

1 Agung, El Chichón, and Pinatubo) where the eruption begins in year 0. DJF (0/1) is peak of the strong  
 2 tropical volcanic forcing composite (Taken from McGregor et al. (2020). © 2018 American Geophysical  
 3 Union, used with permission).



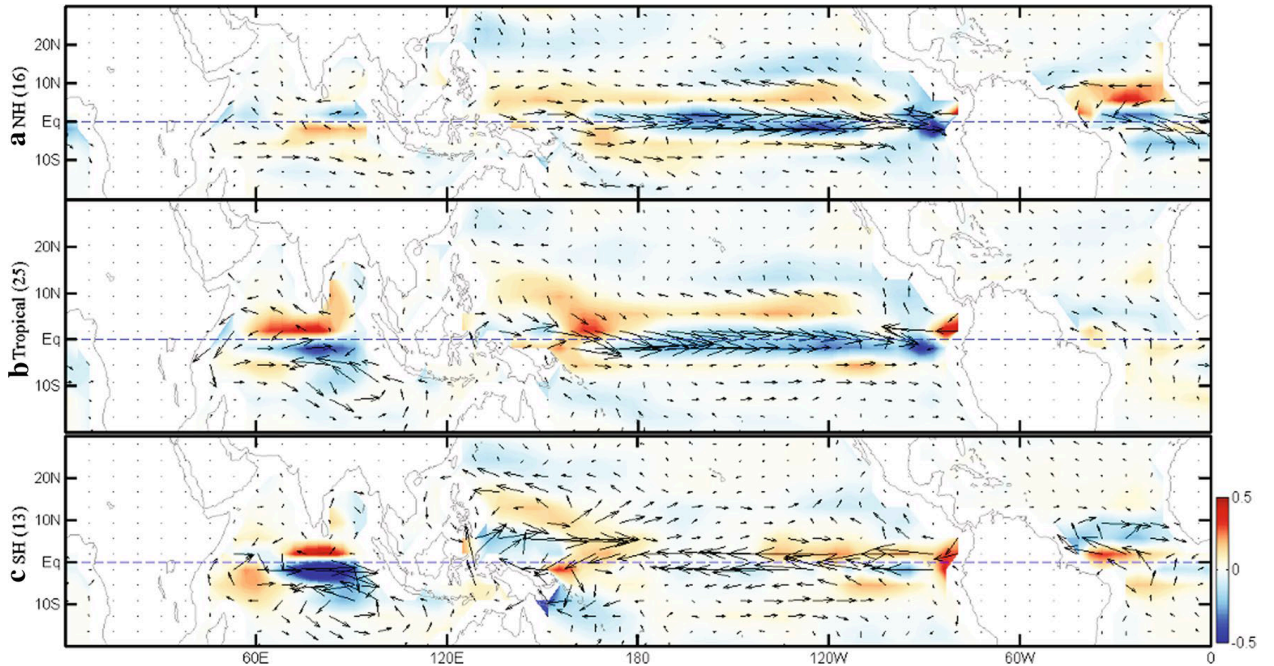
4  
 5 **Figure 6:** Transition to La Niña from tropical eruption-induced El Niño mode and internal El Niño mode.  
 6 Shown are the composite NINO3 index for 25 tropical eruptions during the period 501 to 2000 AD (thick red  
 7 line) and for the El Niño in the control run (thick blue line), as well as the associated zonal wind anomalies  
 8 (dashed lines) averaged over the western Pacific (5°S–5°N, 120°E–150°E). “1” denotes 1 year after each  
 9 eruption, and “2”, 2 years. The El Niño in the control run is defined when the boreal winter (December–  
 10 February average) NINO index is above one standard deviation. Each variable is standardized by its  
 11 maximum value in years “1” and “2”. The year is defined as the eruption year when its annual aerosol is  
 12 larger than the 2 years before and after it. When the eruption starts late in the year, e.g., November or  
 13 December, it has maximum aerosol density in the following year; in such case, the following year is  
 14 considered as the eruption year (Reproduced from Liu et al. (2018) under a creative commons attribution 4.0  
 15 license <https://creativecommons.org/licenses/by/4.0/>).

16  
 17



1  
2  
3  
4  
5  
6  
7  
8

**Figure 7:** CESM version 1.0 (CESM1) model simulated SST anomaly (K) evolution after different eruptions. The composites of normalized 3-month-mean SST anomalies (shading), and 850-hPa wind anomalies (vectors, m/s) since the first winter after the NH (a), the tropical (b), and the SH (c) eruptions. “0” denotes the year of each eruption, and “+1” indicates 1 year after the eruption. During the simulated 1500 years from 501 to 2000 AD, there were 16 NH, 25 tropical, and 13 SH explosive volcanoes (Reproduced from Liu et al. (2018) under a creative commons attribution 4.0 license <https://creativecommons.org/licenses/by/4.0/>).



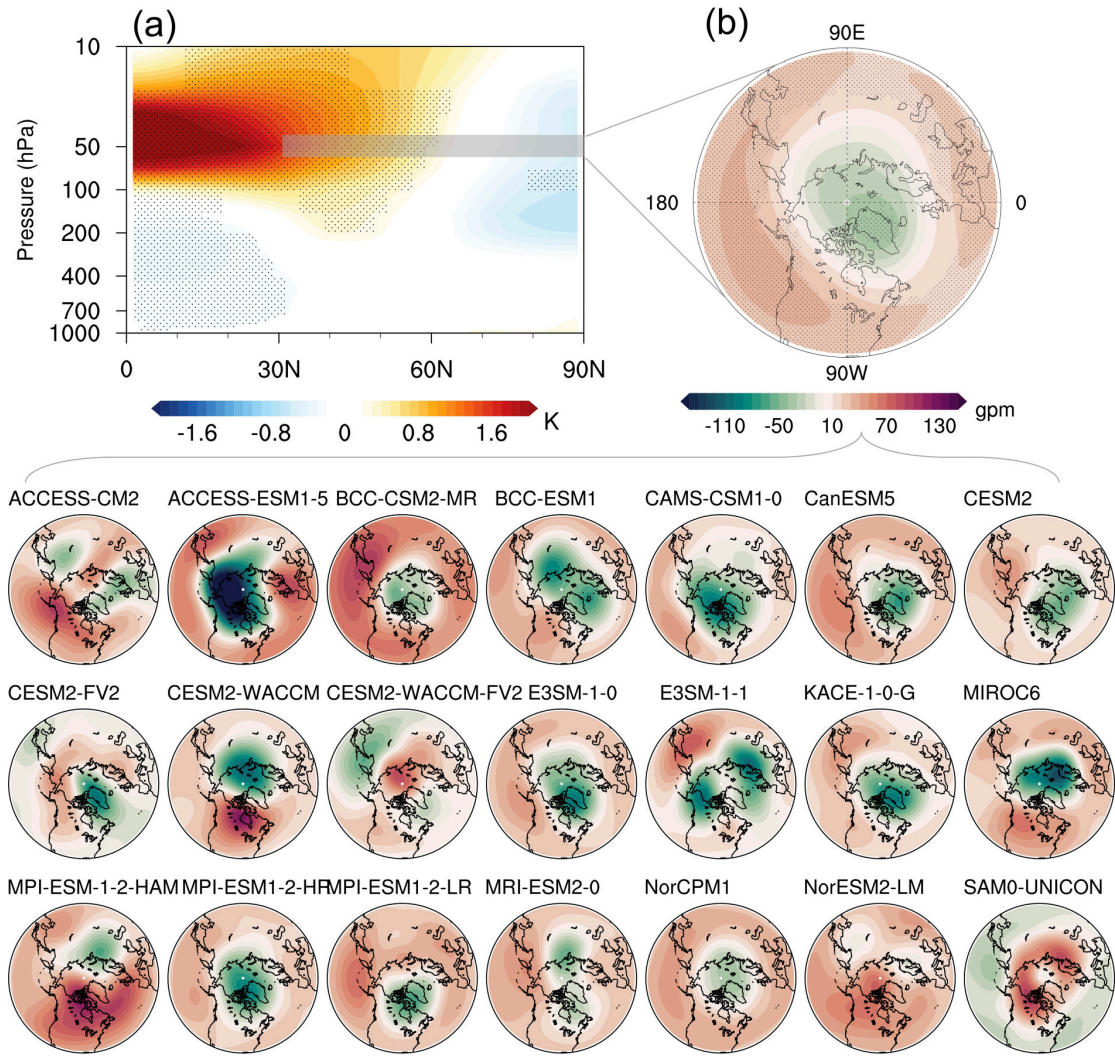
9

10 **Figure 8:** CESM version 1.0 (CESM1) model simulated oceanic responses to different eruptions. The



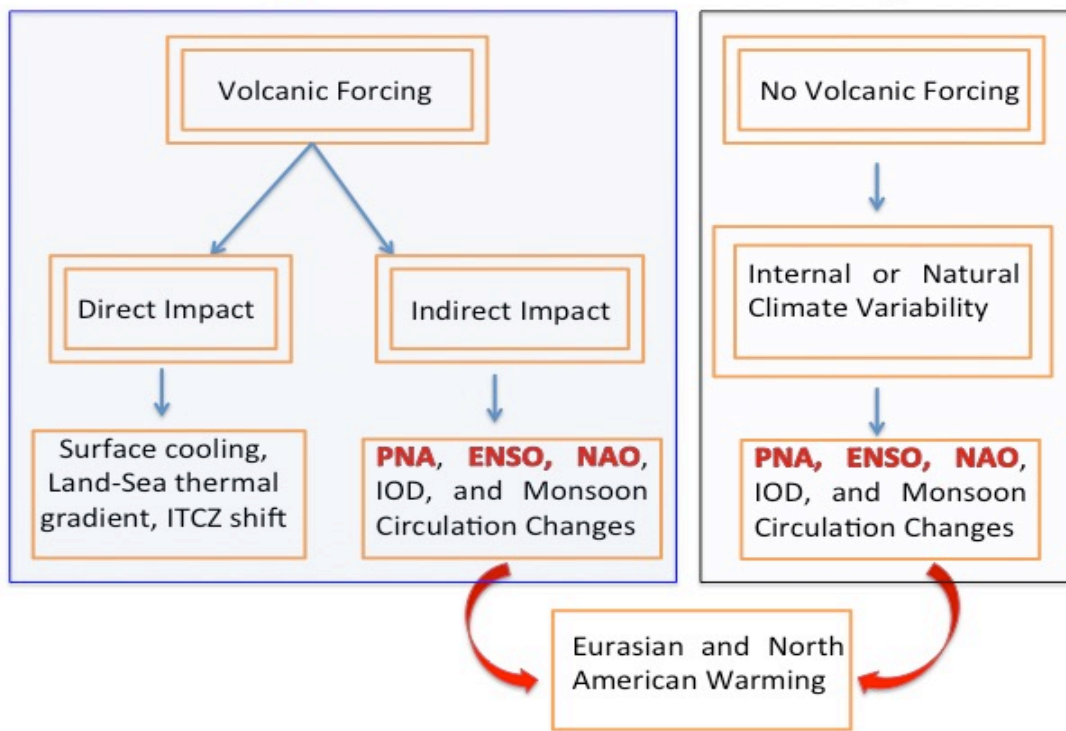
1  
2  
3  
4  
5

normalized composite summer-mean (June–August) surface currents (m/s) and surface (0–20 m) upwelling anomalies (shading, K) one year after the NH (a), the tropical (b), and the SH (c) eruptions (Reproduced from Liu et al. (2018) under a creative commons attribution 4.0 license <https://creativecommons.org/licenses/by/4.0/>).



6  
7  
8  
9  
10  
11  
12  
13  
14  
15  
16  
17

**Figure 9:** Stratospheric responses to tropical volcanism in CMIP6. Composites of (a) zonally averaged temperature anomalies as a function of latitude and height (shading), and (b) 50-hPa geopotential height anomalies in the first NH winter following the five tropical eruptions for the multi-model mean of the 21 CMIP6 models (shading). The ensemble mean of each model is also shown in (b). Stippling denotes anomalies significant at the 95% confidence level (Reproduced from Liu et al. (2020) under a creative commons attribution 4.0 license <https://creativecommons.org/licenses/by/4.0/>).



2 **Figure 10:** A schematic diagram suggesting two experiments using a large number of coupled GCMs with  
 3 large ensemble size with volcanic (i.e., panel A) and non-volcanic forcing (i.e., panel B). The difference of  
 4 the ensemble average of these multi-model, large ensemble volcanic forcing experiments from non-volcanic  
 5 experiments is required to delineate the volcanic impact (i.e., direct and non-direct) from natural climate  
 6 variability. Large-scale circulation changes that supposedly play role in high-latitude winter warming are  
 7 shown in bold red font.

8  
 9  
 10  
 11  
 12  
 13  
 14  
 15  
 16  
 17  
 18  
 19  
 20  
 21